LIMNOLOGY
and
OCEANOGRAPHY

ASLO

Limnol. Oceanogr. 63, 2018, S458–S476

doi: 10.1002/lno.10775

Quantifying nitrate dynamics in a mesotrophic lake using triple oxygen isotopes as tracers

Urumu Tsunogai, * Takanori Miyauchi, Takuya Ohyama, Daisuke D. Komatsu,[a] Masanori Ito, Fumiko Nakagawa
Graduate School of Environmental Studies, Nagoya University, Nagoya, Japan

Abstract

Vertical distributions of both concentrations and stable isotopic compositions of nitrate, including the ^{17}O-excesses ($\Delta^{17}O$), were determined four times during 1 yr within the mesotrophic water column of Lake Biwa in Japan. By using both the deposition rate of atmospheric nitrate onto the entire surface of the lake and the influx/efflux of both atmospheric and remineralized nitrate via streams reported in the literature, we quantified the annual dynamics of nitrate (gross production rate of nitrate through nitrification and gross metabolic rate of nitrate through assimilation and denitrification), together with their seasonal variations, based on the $\Delta^{17}O$ method. The results revealed that 642 ± 113 Mmol (Mmol = 10^6 mol) of the remineralized nitrate was supplied into the water column through nitrification in the lake on an annual basis, while 810 ± 120 Mmol of nitrate was metabolized in the lake through assimilation and denitrification. In addition, it turns out that nitrification was active, not only in the hypolimnion, but also in the epilimnion and upper thermocline in this lake. Furthermore, the total metabolic rates of nitrate varied seasonally, with the highest rates in summer and the lowest in winter. Because the difference between the annual metabolic rate of nitrate estimated based on the $\Delta^{17}O$ method and the annual assimilation rate of nitrate estimated based on the traditional ^{15}N incubation method was only 20%, we concluded that the $\Delta^{17}O$ method reliably estimates the dynamics of nitrate in mesotrophic lakes.

Nitrate (NO_3^-) is a key nutrient in aquatic environments that often limits primary production. Nitrate dynamics in an aquatic environment, i.e., gross production rate of nitrate through nitrification (F_{nit}), gross metabolic rate of nitrate through assimilation (F_{assim}), and gross metabolic rate of nitrate through denitrification (F_{denit}), are important parameters to be quantified when evaluating both the present and future state of the aquatic environment. In most studies that have been conducted to date, nitrate dynamics has been estimated via incubation experiments using ^{15}N tracer techniques. To quantify F_{assim}, for instance, ^{15}N-labeled NO_3^- is added into bottles that simulate in situ conditions of the aquatic environment studied, which leads to the production of particulate organic-^{15}N ($PO^{15}N$) through assimilation over a known incubation period of several hours to several days (Dugdale and Goering 1967; Knap et al. 1996). The $PO^{15}N$ is then gathered and quantified using mass spectrometry.

The experimental procedures using ^{15}N tracer, however, are generally costly and complicated. Besides, while the obtained nitrate dynamics is an instantaneous assimilation rate at the point of observation, such a value may be temporally variable in response to various factors such as changes in temperature, light intensity, nutrients, and community structure. As a result, tedious and time-consuming time series observations are needed to estimate long-term nitrate dynamics (such as annual nitrate dynamics). Furthermore, nitrate dynamics estimated based on bottle incubations often can be inaccurate, because the incubation itself can result in the production of artifacts by changing the physical/chemical environment from that in situ. It is difficult to simulate nitrate dynamics via periphyton or microbes on the lake bottom using bottle incubations (Axler and Reuter 1996). Additionally, the usual ^{15}N tracer methods do not include assimilated nitrogen released to dissolved organic-^{15}N ($DO^{15}N$) during incubation within the estimated assimilation rates (Slawyk et al. 1998).

To estimate both the gross nitrification rate (F_{nit}) and gross metabolic rate of nitrate ($F_{assim} + F_{denit}$) in a lake more

*Correspondence: urumu@nagoya-u.jp

[a]Present address: School of Marine Science and Technology, Tokai University, Shimizu, Shizuoka, Japan

accurately, we proposed a new method using the ^{17}O-excess ($\Delta^{17}O$) of dissolved NO_3^- in the water column of the lake as a tracer (Tsunogai et al. 2011). This simple method ($\Delta^{17}O$ method) overcomes most of the aforementioned problems inherent in the conventional ^{15}N tracer method. Next, we introduce the $\Delta^{17}O$ method briefly.

The natural stable isotopic composition of nitrate consists of $\delta^{15}N$, $\delta^{17}O$, and $\delta^{18}O$, where $\delta^{18}O = R_{sample}/R_{standard} - 1$ and R is the $^{18}O/^{16}O$ ratio (or the $^{17}O/^{16}O$ ratio in the case of $\delta^{17}O$ or the $^{15}N/^{14}N$ ratio in the case of $\delta^{15}N$) for the sample and each international standard (air N_2 for nitrogen and Vienna standard mean ocean water [VSMOW] for oxygen). The atmospheric nitrate ($NO_{3\,atm}^-$) that is produced from atmospheric NO through photochemical reactions can be characterized by the anomalous enrichment in ^{17}O from the other usual nitrate (remineralized nitrate: $NO_{3\,re}^-$) that is produced from organic nitrogen through general chemical reactions including microbial nitrification in the biosphere (Michalski et al. 2004). Because the oxygen atoms of $NO_{3\,re}^-$ are derived from either terrestrial O_2 or H_2O via usual chemical reactions such as microbial nitrification (Aleem et al. 1965; Andersson and Hooper 1983; Kumar et al. 1983), $NO_{3\,re}^-$ shows mass-dependent relative variations between $^{17}O/^{16}O$ and $^{18}O/^{16}O$ ratios. On the other hand, only unprocessed $NO_{3\,atm}^-$ displays an anomalous enrichment in ^{17}O from the mass-dependent relative variations, reflecting oxygen atom transfers from anomalously ^{17}O enriched ozone (O_3) during the conversion of NO_x to $NO_{3\,atm}^-$ (Michalski et al. 2003; Morin et al. 2008; Tsunogai et al. 2010). By using the $\Delta^{17}O$ signature (the magnitude of ^{17}O excess) defined by the following equation (Miller 2002; Kaiser et al. 2007), we can distinguish unprocessed $NO_{3\,atm}^-$ (showing $\Delta^{17}O$ around $+26‰$ in mid-latitude: Tsunogai et al. 2016) from $NO_{3\,re}^-$ (showing $\Delta^{17}O$ close to $0‰$):

$$\Delta^{17}O = \frac{1+\delta^{17}O}{(1+\delta^{18}O)^{\beta}} - 1, \quad (1)$$

where the constant β is 0.5279 (Miller 2002; Kaiser et al. 2007).

Continuous monitoring of the $\Delta^{17}O$ value of $NO_{3\,atm}^-$ deposited at mid-latitudes has clarified that the annual averages of $\Delta^{17}O$ values of $NO_{3\,atm}^-$ are relatively the same every year (Michalski et al. 2003; Kaiser et al. 2007; Alexander et al. 2009; Tsunogai et al. 2010, 2016). In addition, $\Delta^{17}O$ is nearly stable during the mass-dependent isotope fractionation processes within surface ecosystems (Miller 2002; Michalski et al. 2004; Nakagawa et al. 2013). Therefore, although the $\delta^{15}N$ or $\delta^{18}O$ signature of $NO_{3\,atm}^-$ can be overprinted by biogeochemical processes subsequent to deposition, $\Delta^{17}O$ can be used as a robust tracer of unprocessed $NO_{3\,atm}^-$ to reflect the mole fraction of unprocessed $NO_{3\,atm}^-$ within total NO_3^-, regardless of partial metabolism through denitrification and assimilation subsequent to deposition (Michalski et al. 2004; Tsunogai et al. 2011, 2014).

As a result, the average $\Delta^{17}O$ value of nitrate in a lake's water column ($\Delta^{17}O_{lake}$) should reflect the long-range average relative supply rate between $NO_{3\,atm}^-$ and $NO_{3\,re}^-$ prior to the observation (Tsunogai et al. 2011). That is to say, by determining $\Delta^{17}O_{lake}$ in a lake where we can omit the influence of influx/efflux of nitrate via rivers, we can express the average supply rate of $NO_{3\,re}^-$ through nitrification in the lake's water column (F_{nit}) as a function of the average supply rate of nitrate through atmospheric deposition (F_{atm}). In addition, assuming steady-state conditions in the lake, we can express the total metabolic rate of nitrate through assimilation and denitrification ($F_{assim} + F_{denit}$) as a function of the average supply rate of nitrate through atmospheric deposition (F_{atm}) as well.

The deposition rate of $NO_{3\,atm}^-$ (F_{atm}) has been monitored extensively at many observation sites worldwide because of the problem of transboundary air pollution (EANET 2014; Vet et al. 2014), and the data generated from such can be employed to estimate the precise deposition rate of $NO_{3\,atm}^-$ onto individual aquatic environments (F_{atm}), at least in eastern Asia (EANET 2014). Using both the $\Delta^{17}O_{lake}$ value determined for Lake Mashu, an oligotrophic lake in northern Japan (Fig. 1a), and the rate at which $NO_{3\,atm}^-$ is deposited into the lake (F_{atm}), Tsunogai et al. (2011) estimated both the average nitrification rate (F_{nit}) and average assimilation rate of nitrate (F_{assim}) in the lake successfully, assuming that the metabolic rate of nitrate through denitrification (F_{denit}) was much less than F_{assim} in the highly oxic lake. Recent progress in the use of ^{15}N tracer methods to determine the gross in vitro nitrification rate has been remarkable (Santoro et al. 2010). However, the $\Delta^{17}O$ method represents a simple and accurate alternative technique to determine in situ values for both the gross nitrification rate and gross metabolic rate of nitrate in freshwater and marine environments that contain detectable quantities of $NO_{3\,atm}^-$ within the total nitrate pool in the water column (Tsunogai et al. 2011).

Lake Mashu, however, is a subalpine, oligotrophic crater lake with no perennial inflows/outflows and a long residence time for the water of more than 100 yr. Most of the catchment is occupied by the lake surface so the influx/efflux of nitrate (not only total nitrate but also $NO_{3\,atm}^-$) via rivers can be omitted from the calculations. To apply the $\Delta^{17}O$ method in lakes in general for the accurate determination of the nitrate dynamics where substantial quantities of nitrate could have been supplied/removed through inflows/outflows, additional corrections are needed.

Besides, to apply the $\Delta^{17}O$ method in lakes, detectable quantities of $NO_{3\,atm}^-$ must be contained within the total nitrate pool. Whereas the water of oligotrophic Lake Mashu contained detectable quantities of $NO_{3\,atm}^-$ within the total nitrate pool (the average mixing ratio of $NO_{3\,atm}^-$ within total nitrate was $9.7\% \pm 0.8\%$; Tsunogai et al. 2011), a smaller mixing ratio can be anticipated for mesotrophic/eutrophic environments.

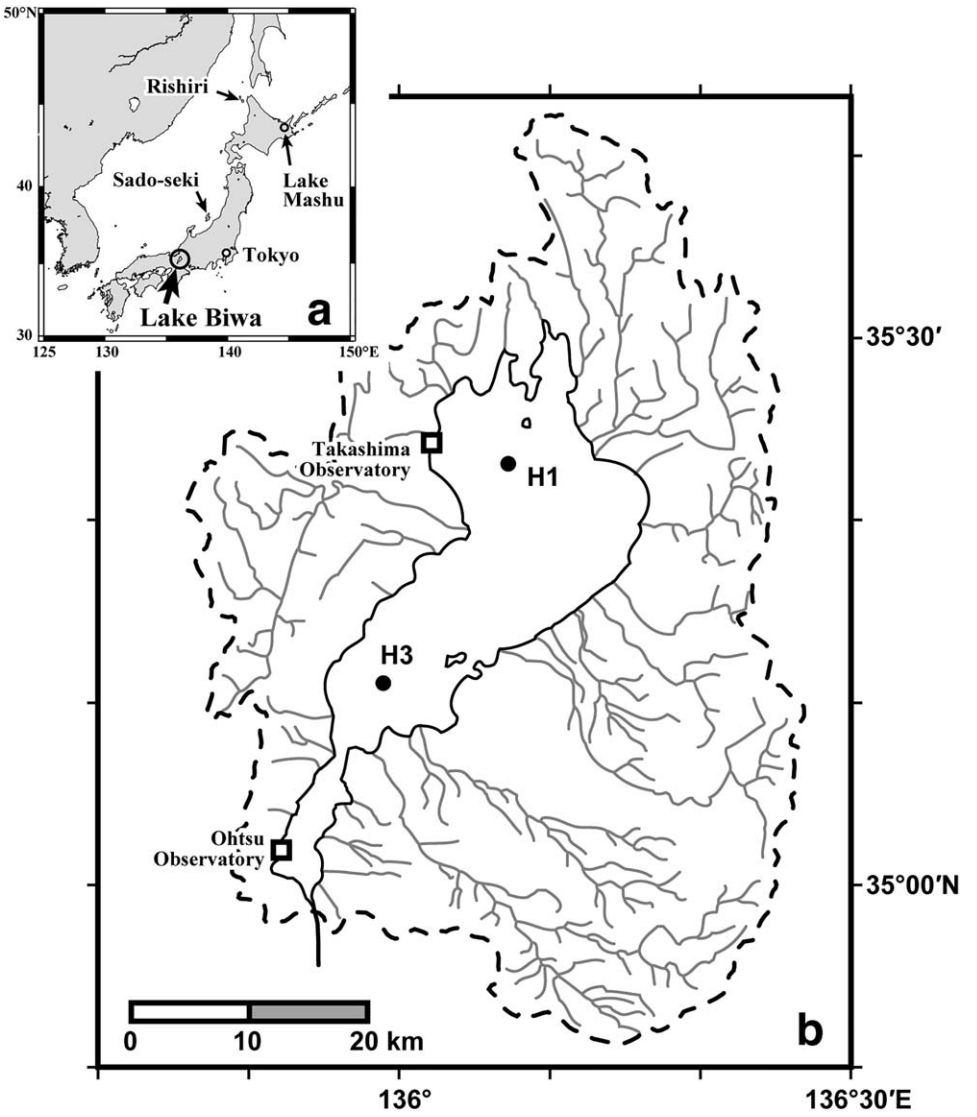

Fig. 1. Map showing the location of Lake Biwa in Japan (**a**). Locations of water sampling stations (black circles) and observatories for the deposition rate of atmospheric nitrate (white squares) in and around Lake Biwa (modified from Ohte et al. 2010) (**b**). The dashed line corresponds to the boundary of the Lake Biwa watershed.

To confirm that we can quantify nitrate dynamics (F_{nit} and $F_{assim} + F_{denit}$) in lakes that are more general with inflows and outflows using the $\Delta^{17}O$ method, the stable isotopic compositions of nitrate, including the $\Delta^{17}O$ values, were determined four times during 1 yr in the water column of mesotrophic Lake Biwa, where influx/efflux via inflows/outflows were already determined for both total nitrate and $NO_{3\ atm}^-$ (Table 1) (Tsunogai et al. 2016). In addition to determining the annual nitrate dynamics in the lake, we also deduced the seasonal variation in the dynamics. The quantified nitrate dynamics in the lake were applied to clarify the reasons for the remarkable biogeochemical features found in the lake, such as rapid removal of P nutrients to sediments (Tezuka 1986; Yoshimizu et al. 2002). The fate of $NO_{3\ atm}^-$ deposited onto the hydrosphere in general (Duce et al. 2008; Elser et al. 2009) were clarified through these studies as well. Furthermore, we also conducted traditional incubation experiments using the ^{15}N tracer method to obtain independent measurements of the gross assimilation rate (F_{assim}) to evaluate whether the $\Delta^{17}O$ method could be used to obtain reliable nitrate dynamics.

Experimental section

Site description

Lake Biwa, located in the central part of the Japanese Islands, is the largest freshwater lake in Japan (Fig. 1). It has a surface area of 670.4 km^2, a total catchment area of 3174 km^2, and annual precipitation of around 2000 mm. More than 120 rivers flow into the lake, but the Seta River at

Table 1. The gross influx/efflux of total nitrate (ΔN) and atmospheric nitrate (ΔA) via inflows/outflows used in the calculations during each observation interval (unit Mmol = 10^6 mol), together with the flux-weighted average $\delta^{15}N$, $\delta^{18}O$, and $\Delta^{17}O$ values of total nitrate in the inflows/outflows during each interval (Tsunogai et al. 2016).

	Spring (n = 1–2)	Summer (n = 2–3)	Autumn (n = 3–4)	Winter (n = 4–5)	Annual (n = 1–5)
Duration (d)	**94**	**49**	**77**	**145**	**365**
Inflow					
ΔN_{in}† (M mol)	69 ± 14	3 ± 1	13 ± 3	114 ± 23	199 ± 40
ΔA_{in}† (M mol)	6.4 ± 1.3	0.1	0.8 ± 0.2	2.8 ± 0.6	10.1 ± 2.0
10^3 $\delta^{15}N$*	+4.0	+6.8	+5.6	+5.6	+5.1
10^3 $\delta^{18}O$*	+6.1	−0.8	+3.3	−1.5	+1.4
10^3 $\Delta^{17}O$*	+2.5	+0.8	+1.7	+0.6	+1.3
Outflow					
ΔN_{out}† (M mol)	24 ± 5	6 ± 1	5 ± 1	32 ± 6	67 ± 13
ΔA_{out}† (M mol)	1.4 ± 0.1	0.1	0.2	0.4 ± 0.1	2.2 ± 0.4
10^3 $\delta^{15}N$*	+7.3	+11.4	+10.4	+18.0	+13.1
10^3 $\delta^{18}O$*	+3.4	+4.8	+3.0	−0.7	+1.5
10^3 $\Delta^{17}O$*	+1.6	+0.4	+1.4	+0.4	+0.9

* The flux-weighted average values estimated from (1) flow rates of water, (2) nitrate concentrations, and (3) $\delta^{15}N$, $\delta^{18}O$, and $\Delta^{17}O$ values of nitrate, determined at 32 major inflows and one major outflow in Lake Biwa on four occasions in 2013 (Tsunogai et al. 2016).

† Total influx/efflux of N (NO_3^-) or A ($NO_{3\,atm}^-$) estimated from (1) flux-weighted average nitrate concentrations in the inflows/outflows determined by Tsunogai et al. (2016), (2) flux-weighted average $\Delta^{17}O$ value of nitrate in the inflows/outflows determined by Tsunogai et al. (2016), and (3) total influx/efflux of water determined by other researchers and compiled by Tsunogai et al. (2016), in which both influx of water via streams and influx of water via groundwater were included.

the southern end of the lake, also known as the Yodo River, is the only natural outflow. The main basin of Lake Biwa is mesotrophic. Thermal stratification is present in the lake from May to December, and vertical water convection to the bottom of the lake occurs regularly from January to April. The average depth and water residence time of the basin are 43 m and 5.5 yr, respectively. The depth of the euphotic zone during the stratified season ranges from 10 m to 21 m, with an average of 15 m (Urabe et al. 1999).

Similar to many lakes worldwide, Lake Biwa has been experiencing eutrophication. The increase in nutrient loading, especially of P nutrients, due to urbanization around the lake started in the 1960s, and blooms of *Uroglena americana* have occurred since 1977 and blooms of cyanobacteria since 1983 (Hsieh et al. 2011). As a result of water treatment regulations in 1982, however, nutrient loading has been progressively reduced (Hsieh et al. 2011). Still, we can find many environmental problems related to eutrophication in the lake. To clarify the pathways and origins of the nitrate supplied into the lake, both concentrations and stable isotopic compositions ($\delta^{15}N$, $\delta^{18}O$, and $\Delta^{17}O$) of dissolved nitrate were determined in the major inflows/outflows of the lake (Tsunogai et al. 2016). Based on these values, Tsunogai et al. (2016) estimated the gross influx/efflux of total nitrate (ΔN) and $NO_{3\,atm}^-$ (ΔA) via inflows/outflows and groundwater during each observation interval, together with the average $\delta^{15}N$, $\delta^{18}O$, and $\Delta^{17}O$ values of total nitrate in the inflows/outflows (Table 1).

Sampling

Lake water was collected during four sampling campaigns in 2013, on 15 March, 17 June, 05 August, and 21 October, which are the same days river water sampling occurred as described by Tsunogai et al. (2016), from the research vessel HASU (Center for Ecological Research, Kyoto University). A 5 L Niskin sampler was used to collect the lake water samples every 5 m (shallow) to 20 m (deep) depth at locations nearby the Imazu central station (Sta. H1 in Fig. 1b; 35°23′41″ N, 136°7′57″ E; depth = 85 m) and the Minami-hira central station (Sta. H3 in Fig. 1b; 35°11′39″ N, 135°59′39″ E; depth = 65 m). Sta. H1 and H3 correspond to the monthly lake water monitoring Sta. 17B and 12B, respectively, of the Lake Biwa Environmental Research Institute (LBERI). Vertical profiles of temperature and conductivity were determined at the stations simultaneously by use of sensors (Sea-bird SBE911plus).

Each sample was transferred into a dark 250–500 mL polyethylene bottle that was prerinsed at least twice with sample water and subsequently stored under refrigeration (4°C) on the boat. Then, the samples were filtered through a precombusted Whatman GF/F filter with a 0.7 μm pore size within 3 h after collection at a shore-based laboratory, and the filtrate was stored in a different dark polyethylene bottle under refrigeration until analysis. Additionally, the seston that was collected on each filter was washed with Milli-Q water, placed in a plastic case, and then stored in a deep freezer (−80°C) for later analyses of the particulate organic nitrogen (PON).

In this study, we defined the sampling number n, where $n = 1$, 2, 3, and 4, as representing the sampling in March, June, August, and October, respectively. In addition, we defined one more hypothetical sampling number ($n = 5$) set exactly 1 yr later than the $n = 1$ date. Please note that there are no data for sampling $n = 5$. The sampling numbers were needed to calculate both annual average and seasonal variation of nitrate dynamics in the lake, by regarding the intervals between $n = 1$ and $n = 2$, $n = 2$ and $n = 3$, $n = 3$ and $n = 4$, $n = 4$ and $n = 5$, $n = 1$ and $n = 5$, as spring, summer, autumn, winter, and 1 yr, respectively, for the lake water in this study.

^{15}N tracer incubation

We also determined the gross assimilation rate of nitrate in the lake's water column based on traditional bottle incubation experiments using a ^{15}N tracer (Dugdale and Goering 1967; Knap et al. 1996; Konno et al. 2010). On the boat, lake water samples collected at the depths of 0 m and 10 m were transferred into 250 mL clear polycarbonate bottles with septum caps (samples were collected at least in duplicate for each depth). Then, 0.3–0.5 mL of 1 mmol L^{-1} $K^{15}NO_3$ solution (10.4 atom%; Shoko, Tokyo, Japan) was added into each incubation bottle at the shore-based laboratory within a maximum of 3 h after collection. The bottles were gently shaken and then incubated in thermostatic baths (7°C, 21°C, 28°C, and 20°C in March, June, August, and October, respectively) on the shore for 24 h while covered with screens to simulate the in situ light intensity. In addition, water samples without ^{15}N tracer added were incubated in a similar manner. Immediately after the incubation period, the seston in each incubated water sample was collected and washed with Milli-Q water on a precombusted Whatman GF/F filter via gentle vacuum filtration (Konno et al. 2010). The obtained filters were then frozen in a deep freezer (−80°C) until analysis.

Analysis

The concentrations of nitrate (NO_3^-) and nitrite (NO_2^-) in each filtrate sample were measured using ion chromatography (Prominence HIC-SP, Shimadzu, Japan) within a few days after each sampling event. The error (standard error of the mean) in the determined concentrations of nitrate was ± 3%. The $\delta^{18}O$ values of H_2O in the samples were analyzed using the cavity ring-down spectroscopy method by employing an L2120-i instrument (Picarro, Santa Clara, California, U.S.A.) equipped with an A0211 vaporizer and autosampler; the error (standard error of the mean) in this method was ± 0.1‰. Both the VSMOW and standard light Antarctic precipitation were used to calibrate the values to the international scale. Then, we determined the stable isotopic compositions of nitrate for the samples, except for the lake surface samples (0–10 m depths) that were taken in August and showed nitrate concentrations less than 1.0 μmol L^{-1}.

To determine the stable isotopic compositions, nitrate in each filtrate sample was chemically converted to N_2O by using a method originally developed to determine the $^{15}N/^{14}N$ and $^{18}O/^{16}O$ ratios of seawater and freshwater nitrate (Mcilvin and Altabet 2005) that was later modified (Tsunogai et al. 2008; Konno et al. 2010; Yamazaki et al. 2011). In brief, the procedures were as follows. Approximately 10 mL of each sample solution was pipetted into a vial with a septum cap. Then, 0.5 g of spongy cadmium was added, followed by 150 μL of a 1 M $NaHCO_3$ solution. The sample was then shaken for 18–24 h at a rate of 2 cycles s^{-1}. Then, the sample solution was decanted into a different vial with a septum cap. After purging the solution using high purity helium, 0.4 mL of an azide/acetic acid buffer was added. After 45 min, the solution was alkalinized by adding 0.2 mL of 6 M NaOH.

Then, the stable isotopic compositions ($\delta^{15}N$, $\delta^{18}O$, and $\Delta^{17}O$) of the N_2O in each vial were determined by using the continuous-flow isotope ratio mass spectrometry (CF-IRMS) system at Nagoya University. This system consists of an original helium purge and trap line, a gas chromatograph (Agilent 6890), a Finnigan MAT 252 mass spectrometer (Thermo Fisher Scientific, Waltham, Massachusetts, U.S.A.) with a modified Combustion III interface (Tsunogai et al. 2000, 2002, 2005; Nakagawa et al. 2004), and a specially designed multicollector system (Komatsu et al. 2008). For each analysis, aliquots of N_2O were introduced, purified using PoraPLOT-Q capillary column (50 m long, 0.32 mm i.d.) held at 30°C, and carried continuously into the mass spectrometer via an open split interface, in which the isotopologues of N_2O^+ at m/z ratios of 44, 45, and 46 were monitored to determine δ^{45} and δ^{46} (Komatsu et al. 2008; Hirota et al. 2010). Each analysis was calibrated by using 99.999% N_2O as a machine-working reference gas. This gas was introduced into the mass spectrometer via an open split interface according to a specific schedule to correct for subdaily temporal variations in the mass spectrometry process. In addition, a working-standard gas mixture containing a known concentration of N_2O, ca. 1000 ppm N_2O in air, was injected from a sampling loop and analyzed in the same manner as that of the samples at least once a day to correct for daily temporal variations in the mass spectrometry process.

Following the analyses based on N_2O^+ monitoring, an additional aliquot of N_2O was introduced to determine the $\Delta^{17}O$ of N_2O (Komatsu et al. 2008). By using the same procedures as those used in the N_2O^+ monitoring mode, purified N_2O was introduced into our original gold tube unit (Komatsu et al. 2008), which was held at 780°C for the thermal decomposition of N_2O to N_2 and O_2. The produced O_2, purified from N_2 using RT-Msieve 5A PLOT capillary column (5 m long, 0.32 mm i.d.) held at 30°C, was then subjected to CF-IRMS to determine the δ^{33} and δ^{34} values by simultaneous monitoring of O_2^+ isotopologues at m/z ratios of 32,

33, and 34. Each analysis was calibrated with 99.999% O_2 gas in a cylinder as a machine-working reference gas which was introduced into the mass spectrometer via an open split interface according to a specific schedule to correct for subdaily temporal variations in the mass spectrometry process. In addition, a working-standard gas mixture containing N_2O of known concentration, ca. 1000 ppm N_2O in air, was analyzed in the same manner as that of the samples at least once a day to correct for daily temporal variations in the mass spectrometry process.

The obtained values of $\delta^{15}N$, $\delta^{18}O$, and $\Delta^{17}O$ for the N_2O derived from the nitrate in each sample were compared with those derived from our local laboratory nitrate standards, which had been calibrated using USGS-34 ($\delta^{15}N = -1.8‰$, $\delta^{18}O = -27.93‰$, $\Delta^{17}O = +0.04‰$) and USGS-35 ($\delta^{15}N = +2.7‰$, $\delta^{18}O = +57.5‰$, $\Delta^{17}O = +20.88‰$) (Böhlke et al. 2003; Kaiser et al. 2007) to calibrate the values of the sample nitrate to an international scale and to correct for both isotope fractionation during the chemical conversion to N_2O and the progress of oxygen isotope exchange between the nitrate-derived reaction intermediate and water (ca. 20%). In this study, we adopted the internal standard method (Nakagawa et al. 2013; Tsunogai et al. 2014) for the calibrations of sample NO_3^-.

To determine whether samples were deteriorated or contaminated during storage and whether the conversion rate from nitrate to N_2O was sufficient, the concentrations of nitrate in the samples were determined each time we analyzed isotopic compositions using CF-IRMS based on the N_2O^+ or O_2^+ outputs. We adopted the $\delta^{15}N$, $\delta^{18}O$, or $\Delta^{17}O$ values only when concentrations measured via CF-IRMS correlated with those measured via ion chromatography just after the sampling within a difference of 10%. About 10% of the whole isotope analyses showed conversion efficiencies lower than this criterion. The nitrate in these samples was converted to N_2O again and reanalyzed for the stable isotopic compositions. None of the samples showed significant nitrate deterioration or nitrate contamination during storage.

We repeated the analyses of the $\delta^{15}N$, $\delta^{18}O$, and $\Delta^{17}O$ values of nitrate for each sample at least three times to attain better precision. Most of the samples had a nitrate concentration of more than 5.0 μmol L^{-1}, which corresponded to a nitrate quantity greater than 50 nmol in a 10 mL sample. This amount was sufficient for determining the $\delta^{15}N$, $\delta^{18}O$, and $\Delta^{17}O$ values with the highest precision of our CF-IRMS system. For cases when the nitrate concentration was less than 5.0 μmol L^{-1}, the sample volume was increased to 30 mL and the number of analyses was also increased. Thus, all isotopic data presented in this study have an error (standard error of the mean) better than $\pm 0.2‰$ for $\delta^{15}N$, $\pm 0.3‰$ for $\delta^{18}O$, and $\pm 0.1‰$ for $\Delta^{17}O$.

Nitrite (NO_2^-) in the samples interferes with the final N_2O produced from NO_3^- because the chemical method also converts NO_2^- to N_2O (Mcilvin and Altabet 2005). Therefore, it is sometimes necessary to remove NO_2^- prior to converting NO_3^- to N_2O. However, in this study, all the lake water samples analyzed for stable isotopic compositions had NO_2^- concentrations lower than the detection limit (0.05 μmol L^{-1}). Thus, in this study, we skipped the processes for removing NO_2^-.

The concentrations and $\delta^{15}N$ values of PON on the GF/F filters were analyzed using the method developed by Tsunogai et al. (2008). In this method, the organic nitrogen on each filter is oxidized to NO_3^- using persulfate. Subsequent processes to determine the $\delta^{15}N$ values of nitrate were generally the same as those used for the NO_3^- analyses described above. To calibrate the value to the international scale, several local laboratory standards that had been calibrated using internationally distributed isotope reference materials (IAEA N1, USGS 25, and IAEA N2; Böhlke and Coplen 1995) were used for routine calibration purposes by measuring them in the same manner in which the samples were measured. The natural PON data presented in this study had an error of $\pm$ 0.3‰ for $\delta^{15}N$.

Calculation for the nitrate dynamics using $\Delta^{17}O$

First, the total inventory of nitrate in the lake water (N) and its $\delta^{15}N$, $\delta^{18}O$, and $\Delta^{17}O$ values (δ_{lake}) were calculated for each observation n ($n = 1$, 2, 3, and 4) from the data describing their vertical distributions in the water column and the vertical distribution of the area in the lake using the following equations (Tsunogai et al. 2000, 2011):

$$N = \sum_{z=0}^{80} (C_z \times S_z \times \Delta z), \tag{2}$$

$$\delta_{lake} = \frac{\sum_{z=0}^{80} (\delta_z \times C_z \times S_z \times \Delta z)}{N}, \tag{3}$$

where C_z, δ_z, and S_z denote the nitrate concentration, each isotopic value ($\delta^{15}N$, $\delta^{18}O$, and $\Delta^{17}O$), and the area of the lake at depth z, respectively. In this study, we estimated S_z from an electronic online map by the Geospatial Information Authority of Japan (http://maps.gsi.go.jp/).

Because $\Delta^{17}O$ can be used as a robust tracer of unprocessed $NO_{3\,atm}^-$ to reflect the accurate mole fraction of unprocessed $NO_{3\,atm}^-$ within total NO_3^- regardless of partial metabolism through either denitrification and/or assimilation subsequent to deposition, we can relate $\Delta^{17}O$ with the concentrations of $NO_{3\,atm}^-$, $NO_{3\,re}^-$, and NO_3^- in each water sample by using the following equation:

$$\frac{C_{atm}}{C_{total}} = \frac{C_{atm}}{C_{atm} + C_{re}} = \frac{\Delta^{17}O}{\Delta^{17}O_{atm}}, \tag{4}$$

where C_{atm}, C_{re}, and C_{total} denote the concentrations of $NO_{3\,atm}^-$, $NO_{3\,re}^-$, and NO_3^- in each water sample, respectively; and $\Delta^{17}O_{atm}$ and $\Delta^{17}O$ denote the $\Delta^{17}O$ values of $NO_{3\,atm}^-$ and nitrate (total) in each water sample, respectively. Please note that all the NO_3^- other than the unprocessed $NO_{3\,atm}^-$

can be classified into $NO_{3\,re}^-$, including the NO_3^- produced through natural/anthropogenic processes in the biosphere/hydrosphere/geosphere and that stored in soil, fertilizer, manure, sewage, etc. The N nutrients that were originally supplied to the biosphere through atmospheric deposition but then became organic nitrogen through assimilation and eventually NO_3^- via remineralization are classified into $NO_{3\,re}^-$ and not into $NO_{3\,atm}^-$ (Tsunogai et al. 2016).

Because we used the power law (Eq. 1) for the definition of $\Delta^{17}O$, the $\Delta^{17}O$ values are different from those based on the linear definition (Michalski et al. 2002). Please note that our $\Delta^{17}O$ values would have been $0.1 \pm 0.1‰$ higher if we had used the linear definition for calculation. Compared with $\Delta^{17}O$ values based on the linear definition, $\Delta^{17}O$ values based on the power law definition are more stable during mass-dependent isotope fractionation processes. Thus, we used the $\Delta^{17}O$ values of NO_3^- as always stable irrespective of any partial metabolism subsequent to deposition, such as assimilation or denitrification. On the other hand, $\Delta^{17}O$ values based on the power law definition are not conserved during mixing processes between fractions having different $\Delta^{17}O$ values, so the C_{atm}/C_{total} ratios estimated using Eq. 4 are somewhat deviated from the actual C_{atm}/C_{total} ratios in the samples (Tsunogai et al. 2016). However, in this study, the extent of the deviations of the C_{atm}/C_{total} ratios of the lake water NO_3^- was less than 0.15%, therefore, we disregarded this effect in the discussion.

By substituting $\Delta^{17}O_{lake}$ estimated from Eq. 3 for $\Delta^{17}O$ in Eq. 4, the inventory of $NO_{3\,atm}^-$ in the lake water (A) at the initial ($t = 0$) and final ($t = t$) observation times can be estimated from the inventory of NO_3^- in the lake (N) using the following equations:

$$\frac{A_0}{N_0} = \frac{(\Delta^{17}O_{lake})_0}{\Delta^{17}O_{atm}}, \quad (5)$$

$$\frac{A_t}{N_t} = \frac{(\Delta^{17}O_{lake})_t}{\Delta^{17}O_{atm}}, \quad (6)$$

where A_0 and A_t denote the initial and final inventory of $NO_{3\,atm}^-$ in the lake, respectively; N_0 and N_t denote the initial and final inventory of NO_3^- in the lake, respectively; and $(\Delta^{17}O_{lake})_0$ and $(\Delta^{17}O_{lake})_t$ denote the initial and final $\Delta^{17}O_{lake}$, respectively. The relationships between A_0, A_t, N_0, and N_t are schematically shown in Fig. 2, in which we divide the supply/removal processes into river input/output, atmospheric deposition, in-lake nitrification, and in-lake metabolism through assimilation and denitrification.

Because the $\Delta^{17}O$ value of NO_3^- is nearly stable during the partial metabolism of NO_3^- through assimilation and denitrification, the left-hand side of Eq. 6 can be replaced by using the gross amount of NO_3^- supplied/removed through inflows/outflows, atmospheric deposition (ΔN_{atm}), and nitrification in the lake (ΔN_{nit}), as well as the initial inventories of $NO_{3\,atm}^-$ (A_0) and NO_3^- (N_0) in the lake, as shown in the following equations:

$$\frac{A_0 + \Delta A_{in} - \Delta A_{out} + \Delta N_{atm}}{N_0 + \Delta N_{in} - \Delta N_{out} + \Delta N_{atm} + \Delta N_{nit}} = \frac{(\Delta^{17}O_{lake})_t}{\Delta^{17}O_{atm}}, \quad (7)$$

$$\frac{\Delta A_{in}}{\Delta N_{in}} = \frac{\Delta^{17}O_{in}}{\Delta^{17}O_{atm}}, \quad (8)$$

$$\frac{\Delta A_{out}}{\Delta N_{out}} = \frac{\Delta^{17}O_{out}}{\Delta^{17}O_{atm}}, \quad (9)$$

where $\Delta^{17}O_{in}$ and $\Delta^{17}O_{out}$ denote the flux-weighted average $\Delta^{17}O$ values of NO_3^- in the inflows and outflows, respectively; ΔN_{in} and ΔA_{in} denote the gross amount of NO_3^- and $NO_{3\,atm}^-$ being supplied via inflows, respectively; and ΔN_{out} and ΔA_{out} denote the gross amount of NO_3^- and $NO_{3\,atm}^-$ being removed via outflows, respectively, during the interval between the initial ($t = 0$) and final ($t = t$) observation periods.

In estimating the inventories of $NO_{3\,atm}^-$ (A) and thus nitrate dynamics in the Lake Biwa, we used the 3-yr average $\Delta^{17}O$ value of $NO_{3\,atm}^-$ obtained at the Sado-seki monitoring station ($\Delta^{17}O = +26.3‰$; Tsunogai et al. 2016) as the value of $\Delta^{17}O_{atm}$ in Eqs. 4–9, by allowing an error range of 3‰, considering the possible factor changes in $\Delta^{17}O_{atm}$ from the average $\Delta^{17}O$ value as discussed in Tsunogai et al. (2016). About 65% of all the $\Delta^{17}O$ data of $NO_{3\,atm}^-$ obtained at the Sado-seki monitoring station were included in this range of $+26.3 \pm 3.0‰$.

By using Eqs. 7–9, we can obtain ΔN_{nit} for the interval between the initial ($t = 0$) and final ($t = t$) time as follows:

$$\Delta N_{nit} = \frac{(\Delta^{17}O_{lake})_0 - (\Delta^{17}O_{lake})_t}{(\Delta^{17}O_{lake})_t} \times N_0 + \frac{\Delta^{17}O_{atm} - (\Delta^{17}O_{lake})_t}{(\Delta^{17}O_{lake})_t} \times \Delta N_{atm} + \frac{\Delta^{17}O_{in} - (\Delta^{17}O_{lake})_t}{(\Delta^{17}O_{lake})_t} \times \Delta N_{in} - \frac{\Delta^{17}O_{out} - (\Delta^{17}O_{lake})_t}{(\Delta^{17}O_{lake})_t} \times \Delta N_{out}. \quad (10)$$

Then, the gross amount of NO_3^- metabolized totally through assimilation and denitrification in the water column ($\Delta N_{assim} + \Delta N_{denit}$) can be obtained from ΔN_{nit} using the following equation (Fig. 2):

$$\Delta N_{assim} + \Delta N_{denit} = N_0 + \Delta N_{in} - \Delta N_{out} + \Delta N_{atm} + \Delta N_{nit} - N_t \quad (11)$$

By using Eqs. 10, 11, we can estimate both ΔN_{nit} and $\Delta N_{assim} + \Delta N_{denit}$ for each interval between the observations, i.e., spring (interval between $n = 1$ and 2), summer (interval between $n = 2$ and 3), autumn (interval between $n = 3$ and 4), and winter (interval between $n = 4$ and 5). Additionally, we can estimate the annual supply rate of $NO_{3\,re}^-$ through nitrification (F_{nit}) by integrating the whole ΔN_{nit} estimated for each season. We can estimate the annual metabolic rate of NO_3^-

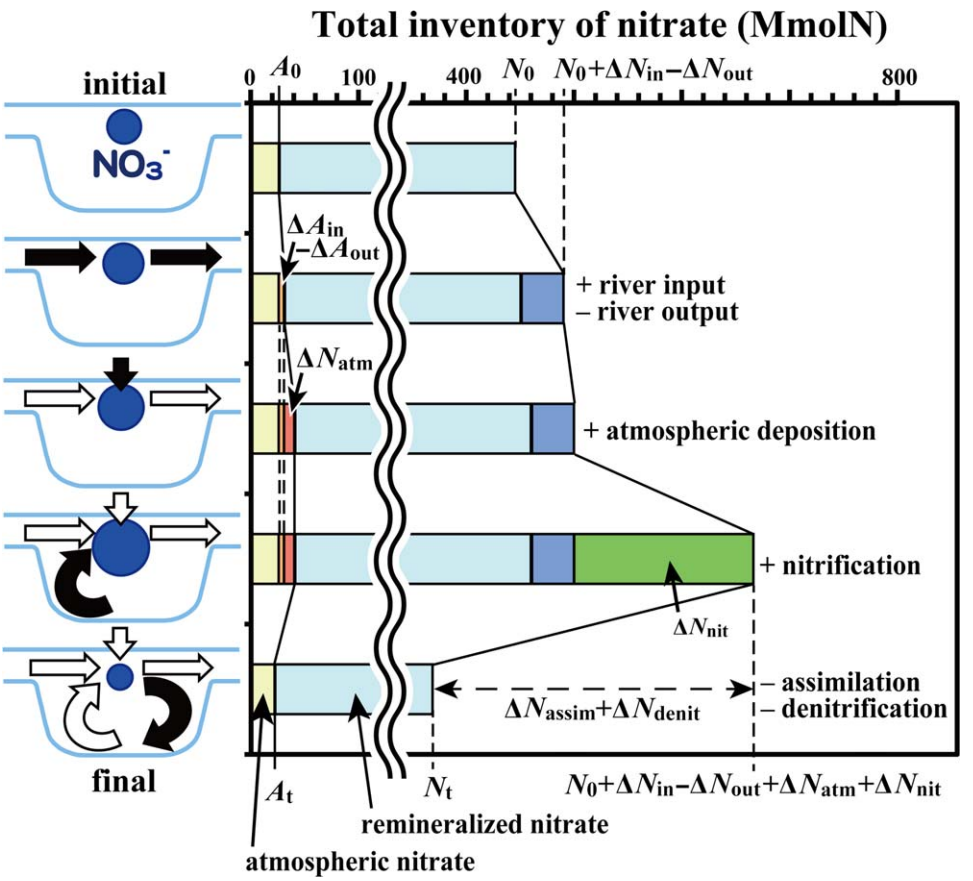

Fig. 2. Schematic diagram showing the temporal variation in the inventory of total nitrate (N) in Lake Biwa, together with that of atmospheric nitrate (*A*). The data were obtained by dividing the supply/removal processes into river input (ΔN_{in}), river output (ΔN_{out}), atmospheric deposition (ΔN_{atm}), in-lake nitrification (ΔN_{nit}), and total metabolism through assimilation and denitrification ($\Delta N_{assim} + \Delta N_{denit}$). The values represented are those that were obtained in March (initial) and June (final) 2013.

through assimilation and denitrification ($F_{assim} + F_{denit}$) as well, by integrating the whole $\Delta N_{assim} + \Delta N_{denit}$ estimated for each season.

To estimate ΔN_{atm} for each interval, we used the areal deposition rate of NO_3^- (wet deposition + dry deposition) determined at the Ohtsu Observatory (Mitamura 2014; Environmental Laboratories Association in Japan 2015), which is located on the southeastern shore of the lake (35°1′35″ N, 135°52′2″ E; Fig. 1b), for the entire surface area of the lake (670.4 km^2). The dry deposition is about 30% of the total deposition (Mitamura 2014). The obtained ΔN_{atm} was 9.5 ± 1.7 Mmol, 4.9 ± 0.9 Mmol, 7.8 ± 1.4 Mmol, and 14.6 ± 2.6 Mmol (Mmol = 10^6 mol) for the spring, summer, autumn, and winter, respectively. The error ranges (about 20%) were estimated from the deviation in the wet deposition rates over a decade at the Ohtsu Observatory from those determined for the Takashima Observatory, located on the northeastern shore of the lake (35°24′21″ N, 136°02′24″ E; Fig. 1b), where only the wet deposition rates were determined for NO_3^- (Shiga Prefecture 2015). As for the values of ΔN_{in}, ΔN_{out}, $\Delta^{17}O_{in}$, and $\Delta^{17}O_{out}$ in each interval, we used those already determined through actual observations of the inflows/outflows (Table 1) (Tsunogai et al. 2016).

Calculation for gross assimilation rates using the ^{15}N tracer method

The gross assimilation rate of NO_3^- in a volume of lake water (V_{assim}) was calculated for each incubation bottle with $^{15}NO_3^-$ addition through comparisons with that without $^{15}NO_3^-$ addition using the following equation:

$$V_{assim} = \frac{\chi_f - \chi_0}{\chi_\Delta - \chi_0} \times [PON]_f \times \frac{1}{t}, \quad (12)$$

where $[PON]_f$ denotes PON content in the bottle with $^{15}NO_3^-$ addition, χ_f denotes $^{15}N/(^{14}N+^{15}N)$ ratios of PON in the bottle with $^{15}NO_3^-$ addition (in atom%), χ_0 denotes $^{15}N/(^{14}N+^{15}N)$ ratios of PON in the bottle without $^{15}NO_3^-$ addition (in atom%), χ_Δ denotes $^{15}N/(^{14}N+^{15}N)$ ratios of NO_3^- in the bottle with $^{15}NO_3^-$ addition (in atom%), and t denotes the duration of the incubation (24 h). Then, each assimilation rate at a particular depth was estimated as the average value of duplicate bottles sampled and incubated simultaneously.

Next, we calculated the areal gross assimilation rate for each observation by integrating the assimilation rates based on volume, whereby we assumed that the data obtained at 0 m and 10 m represented the average values from 0 m to 5 m and from 5 m to 15 m, respectively, and the gross assimilation rates below 15 m were always 0.

Results and discussion

Nitrate in the lake's water column

Our samplings of the lake water were done at two different stations: H1 (depth = 85 m) and H3 (depth = 65 m), which are shown in Fig. 1b. Both concentrations and stable isotopic compositions of NO_3^- showed large vertical and temporal variations that ranged from 0.2 μmol L^{-1} to 21.4 μmol L^{-1} for the concentrations, from +1.7‰ to +10.4‰ for $\delta^{15}N$, from −2.2‰ to +8.3‰ for $\delta^{18}O$, and from +0.7‰ to +2.6‰ for $\Delta^{17}O$. The determined NO_3^- concentrations coincided well with those determined by the Lake Biwa Environmental Research Institute in 2013 (Shiga Prefecture 2015). Moreover, the observed vertical and temporal variations in concentrations were typical of those observed during the past 30 yr (Hayakawa et al. 2012).

Whereas the data showed large variations, the differences between the stations for samples taken at the same depth and observation time were small, i.e., 0.6 μmol L^{-1} for concentrations, 0.7‰ for $\delta^{15}N$, 0.5‰ for $\delta^{18}O$, and 0.2‰ for $\Delta^{17}O$, on average. We concluded that a major part of the lake's water column was horizontally homogeneous. As a result, we used the average values as those representing each depth between 0 m and 60 m and to obtain a single profile for each observation for the depths from 0 m to 80 m in the lake. The obtained profiles are presented in Fig. 3b–e, and these data will be used in further discussions as values representing the whole water column.

In March, the concentrations of NO_3^- were homogenous throughout the water column, at 15.4 μmol L^{-1} (Fig. 3b), which suggests that the water was well mixed vertically in winter. This finding is also supported by the values of $\delta^{15}N$, $\delta^{18}O$, and $\Delta^{17}O$, which were almost uniform in March. Subsequently, the NO_3^- in the surface 10 m decreased to less than 8 μmol L^{-1} in June and to less than 1 μmol L^{-1} in August (Fig. 3b), thus suggesting that active metabolism of NO_3^- occurred, probably through assimilation by phytoplankton during stratification. These results were supported by the ^{15}N and ^{18}O enrichment in the $\delta^{15}N$ and $\delta^{18}O$ values of NO_3^- in the surface 10 m in June when compared with the values in March (Fig. 3d,e), because partial assimilation of NO_3^- by phytoplankton results in residual NO_3^- being enriched with ^{15}N and ^{18}O (Granger et al. 2010).

Although assimilation must have been one of the major processes that controlled both the concentration and isotopic compositions of NO_3^- in the surface layer, we found definite evidence of a trace contribution of new NO_3^- from internal/external sources as well. The maximum $\Delta^{17}O$ value (around +2.3‰) found at the surface in June implied that deposition and accumulation of $NO_{3\,atm}^-$ from the atmosphere at the lake surface occurred during stratification. Meanwhile, the gradual decrease in the $\Delta^{17}O$ value from March to October for the bottom layer (60–80 m) implied that $NO_{3\,re}^-$ remineralized from sinking PON via nitrification had accumulated at the bottom. Thus, while NO_3^- assimilation was the major process that controlled the distribution and temporal variation of NO_3^- in the lake, deposition of $NO_{3\,atm}^-$ on the surface and accumulation of $NO_{3\,re}^-$ through nitrification, at least at the bottom, were also responsible for the distribution and temporal variation of NO_3^- in the lake.

By applying the obtained data to Eqs. 2, 3, we ascertained the values of N, $\delta^{15}N_{lake}$, $\delta^{18}O_{lake}$, and $\Delta^{17}O_{lake}$ for each observation in Table 2. To do so, we assumed that the data obtained at 0 m, 5 m, 10 m, 15 m, 20 m, 40 m, 60 m, and 80 m in March and June represented the average values from 0 m to 2.5 m, 2.5 m to 7.5 m, 7.5 m to 12.5 m, 12.5 m to 17.5 m, 17.5 m to 30 m, 30 m to 50 m, 50 m to 70 m, and 70 m to the bottom, respectively, and those obtained at 0 m, 5 m, 10 m, 15 m, 20 m, 30 m, 40 m, 60 m, and 80 m in August and October represented the average value from 0 m to 2.5 m, 2.5 m to 7.5 m, 7.5 m to 12.5 m, 12.5 m to 17.5 m, 17.5 m to 22.5 m, 22.5 m to 30 m, 30 m to 50 m, 50 m to 70 m, and 70 m to the bottom, respectively. The data divided into shallow (from 0 m to 30 m depth) and deep layers (from 30 m depth to the bottom) are presented as well. For August ($n = 3$), when the NO_3^- concentrations in the surface layers (0 m, 5 m, and 10 m depths) were too low to determine $\delta^{15}N$, $\delta^{18}O$, and $\Delta^{17}O$, we used the values from June ($n = 2$) for calculating $\delta^{15}N_{lake}$, $\delta^{18}O_{lake}$, and $\Delta^{17}O_{lake}$ by assuming that the temporal variations in the values of $\delta^{15}N$, $\delta^{18}O$, and $\Delta^{17}O$ were minimal between June and August. Because the amount of NO_3^- in the surface layers was small in August (about 1.2% of the whole NO_3^- pool in the water column), this assumption had little influence on the final obtained values ($\delta^{15}N_{lake}$, $\delta^{18}O_{lake}$, and $\Delta^{17}O_{lake}$) in August, especially for $\Delta^{17}O_{lake}$, which was an important value for subsequent calculations on the NO_3^- dynamics.

The estimated average $\Delta^{17}O$ values of NO_3^- in the lake ($\Delta^{17}O_{lake}$) were +1.6‰ in March, +1.6‰ in June, +1.2‰ in August, and +1.2‰ in October (Table 2), which corresponded to values for the average mixing ratio of $NO_{3\,atm}^-$ to the inventory of nitrate in the lake of 6.0%, 6.2%, 4.8%, and 4.7%, respectively, using Eq. 5. We concluded that 5.4% ± 0.8% of the inventory of nitrate in the lake originates directly from the atmosphere in the lake's water column; therefore, the remainder of nitrate was of remineralized origin ($NO_{3\,re}^-$) and was produced through nitrification in and around the lake.

The estimated average mixing ratio of $NO_{3\,atm}^-$ to the inventory of NO_3^- in Lake Biwa (5.4% ± 0.8%) was smaller

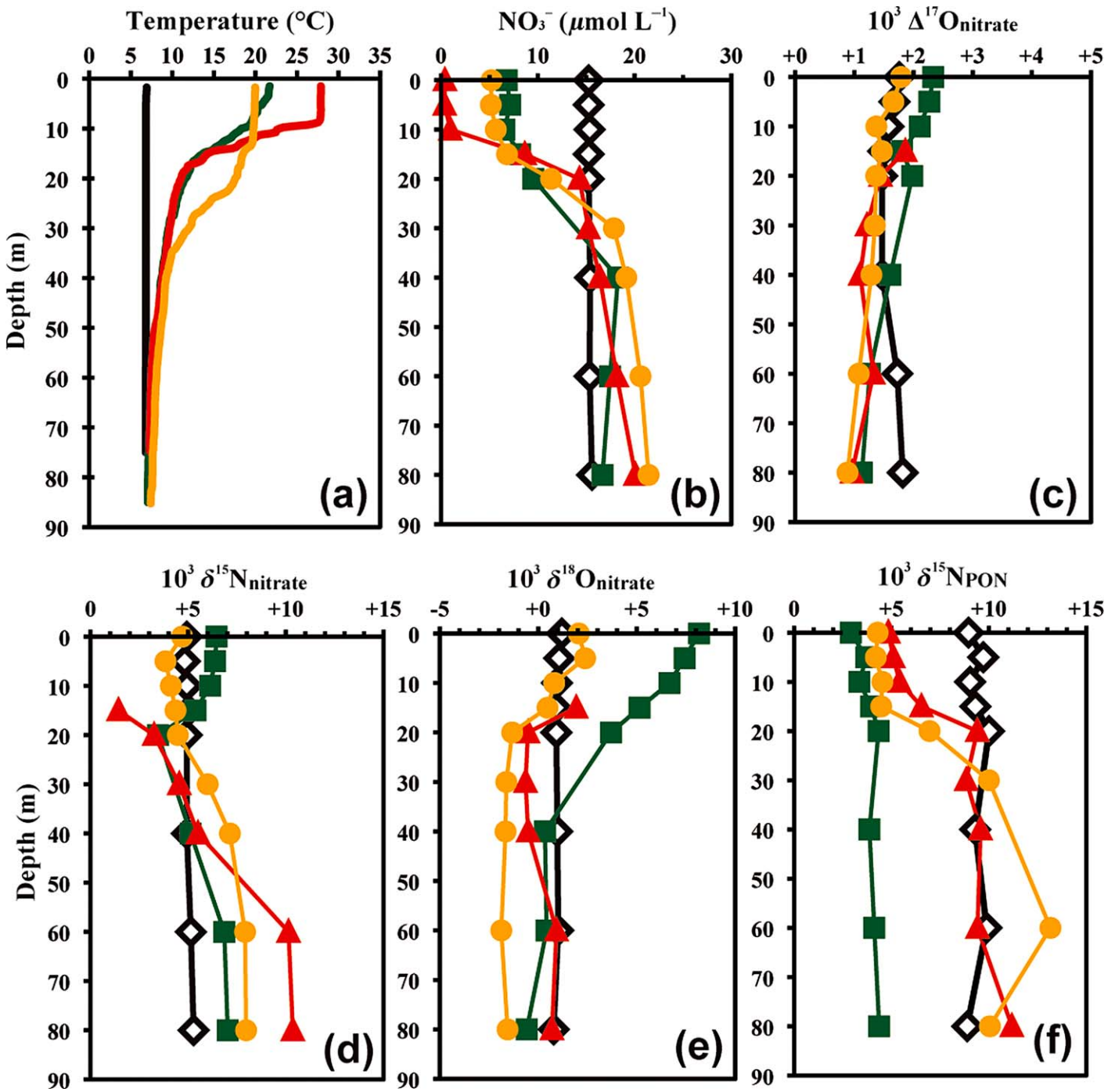

Fig. 3. Vertical distributions of temperature determined at Sta. H1 in March (black), June (green), August (red), and October (yellow) (**a**). Average vertical distributions of the concentration (**b**), $\Delta^{17}O$ (**c**), $\delta^{15}N$ (**d**), and $\delta^{18}O$ (**e**) for nitrate in March (white diamonds), June (green squares), August (red triangles), and October (yellow circles) 2013. Vertical distributions of the $\delta^{15}N$ of PON in the water column (**f**).

than the value determined for the oligotrophic Lake Mashu ($9.7\% \pm 0.8\%$), which was estimated from $\Delta^{17}O$ values as well (Tsunogai et al. 2011). Because the deposition rate of $NO_{3\,atm}^-$ per unit area of the lake surface must be higher in Lake Biwa than in Lake Mashu (EANET 2014), the lower mixing ratios in Lake Biwa imply that there is a larger supply rate of $NO_{3\,re}^-$ to the Lake Biwa water column than that of Lake Mashu. These findings are quantitatively discussed in "Quantifying nitrate dynamics between each observation" section.

Table 2. Temporal variations in the total inventory of nitrate (N), average concentration of nitrate (C_{lake}), average $\delta^{15}N$, $\delta^{18}O$, and $\Delta^{17}O$ for nitrate ($\delta^{15}N_{lake}$, $\delta^{18}O_{lake}$, and $\Delta^{17}O_{lake}$, respectively) in the water column of Lake Biwa, together with the total inventory for atmospheric nitrate (*A*) and remineralized nitrate (*R*). Values divided into shallow (0–30 m depth) and deep layers (30 m to the bottom) are presented in parenthesis as well.

Parameter	Unit	15 March (shallow/deep)	17 June (shallow/deep)	05 August (shallow/deep)	21 October (shallow/deep)
N	Mmol	447	370	348	414
		(231/216)	(121/249)	(102/246)	(134/280)
C_{lake}	μmol L^{-1}	15.3	12.7	12.1	14.4
		(15.3/15.4)	(8.0/17.8)	(6.9/17.5)	(9.0/20.0)
10^3 $\delta^{15}N_{lake}$		+5.0	+5.6	+6.8*	+6.9
		(+4.9/+5.1)	(+4.9/+6.0)	(+4.0*/+7.9)	(+5.4/+7.5)
10^3 $\delta^{18}O_{lake}$		+1.0	+1.9	+0.2*	−1.3
		(+1.0/+1.0)	(+5.4/+0.2)	(+0.3*/+0.2)	(−0.4/−1.7)
10^3 $\Delta^{17}O_{lake}$		+1.6	+1.6	+1.2*	+1.2
		(+1.6/+1.6)	(+2.1/+1.4)	(+1.4*/+1.2)	(+1.4/+1.1)
A	Mmol	27	23	16	19
		(14/13)	(10/14)	(6/11)	(7/12)
R	Mmol	420	347	332	394
		(217/203)	(112/235)	(97/235)	(127/268)

* Estimated using the $\delta^{15}N$, $\delta^{18}O$, and $\Delta^{17}O$ of nitrate in 17 June 2017 for the surface layers (0–10 m depths).

Quantifying nitrate dynamics between each observation

By using the values of *N* and $\Delta^{17}O_{lake}$ for each observation in Table 2, we calculated the gross amount of NO_3^- supplied through nitrification (ΔN_{nit}) as well as that being metabolized through assimilation and denitrification ($\Delta N_{assim} + \Delta N_{denit}$) in the lake by using Eqs. 10, 11 for each interval between the observation times. For the spring season (between 15 March and 17 June sampling), we found that 166 ± 26 Mmol (Mmol = 10^6 mol) of $NO_{3\,re}^-$ had been supplied into the lake water through nitrification, while 297 ± 27 Mmol of NO_3^- had been metabolized in the lake (Table 3). In a similar manner, we also estimated that 216 ± 18 Mmol and 166 ± 29 Mmol of $NO_{3\,re}^-$ had been supplied into the lake water through nitrification during summer season (between 17 June and 05 August sampling) and autumn season (between 05 August and 21 October sampling), respectively, while 245 ± 19 Mmol and 111 ± 30 Mmol of the NO_3^- had been metabolized in the lake. Furthermore, by assuming that the lake returned back to its initial state 1 yr after the first observation in March, we estimated 92 ± 41 Mmol of the $NO_{3\,re}^-$ had been supplied into the lake water through nitrification, while 156 ± 44 Mmol of the NO_3^- had been metabolized in the lake in winter season (between 21 October and 15 March sampling). On a whole year basis, 641 ± 113 Mmol of the $NO_{3\,re}^-$ had been supplied into the lake's water column through nitrification, while 809 ± 120 Mmol of the NO_3^- had been metabolized in the lake through assimilation and denitrification (Table 3; Fig. 4). By dividing each estimated amount by the duration between the observations, we found that the average nitrification rates (F_{nit}) and average metabolic rates of nitrate ($F_{assim} + F_{denit}$) were 1.8 Mmol d^{-1} and 3.2 Mmol d^{-1}, respectively, for spring, 4.4 Mmol d^{-1} and 5.0 Mmol d^{-1} for summer, 2.2 Mmol d^{-1} and 1.4 Mmol d^{-1} for autumn, 0.6 Mmol d^{-1} and 1.1 Mmol d^{-1} for winter, and 1.8 Mmol d^{-1} and 2.2 Mmol d^{-1} for the annual averages. By dividing F_{nit} and $F_{assim} + F_{denit}$ by the surface area (670.4 km^2), we then obtained the average areal nitrification rates and the average areal metabolic rates of 2.6 mmol m^{-2} d^{-1} and 4.7 mmol m^{-2} d^{-1} in spring, respectively, 6.6 mmol m^{-2} d^{-1} and 7.5 mmol m^{-2} d^{-1} in summer, 3.2 mmol m^{-2} d^{-1} and 2.2 mmol m^{-2} d^{-1} in autumn, 0.95 mmol m^{-2} d^{-1} and 1.6 mmol m^{-2} d^{-1} in winter, and 2.6 mmol m^{-2} d^{-1} and 3.3 mmol m^{-2} d^{-1} for the annual averages.

Similar seasonal variation in $F_{assim} + F_{denit}$ of showing a maximum value in summer and a minimum value in winter was detected in Lake Mashu as well (Tsunogai et al. 2011). Past observations on primary production rates in Lake Biwa (F_{assim}) also displayed similar seasonal variation (Yoshimizu et al. 2002; Urabe et al. 2005; Ota et al. 2013). Thus, the observed seasonal variation in $F_{assim} + F_{denit}$, showing a maximum in summer and a minimum in winter, is a highly reasonable estimate for this lake.

Notably, however, the seasonal F_{nit} variation in Lake Biwa was different from that in Lake Mashu. Whereas F_{nit} in Lake Mashu was almost stable regardless of the season (Tsunogai et al. 2011), F_{nit} in Lake Biwa showed significant seasonal variation, with the maximum in summer, and the minimum in winter (Fig. 5). Moreover, F_{nit} in Lake Biwa showed normal correlation with $F_{assim} + F_{denit}$, with a slope close to 1

Table 3. Estimated gross variation in the inventories of atmospheric nitrate (ΔA), remineralized nitrate (ΔR), and total nitrate (ΔN) in the lake divided into each supply/removal process, i.e., (1) atmospheric deposition (Dep), (2) influx via inflows (In) and efflux via outflows (Out), and (3) in-lake nitrification (Nit) and nitrate metabolism through assimilation and denitrification (Metab), in the lake during the observation period. All units are in Mmol N (= 10^6 mol N).

		Spring (94 d)		Summer (49 d)		Autumn (77 d)		Winter (145 d)		Annual (365 d)	
	Process	Supplied	Removed	Supplied	Removed	Supplied	Removed	Supplied	Removed	Supplied	Removed
ΔA	Dep	9.5 ± 1.7	—	4.9 ± 0.9	—	7.8 ± 1.4	—	14.6 ± 2.6	—	36.9 ± 6.7	—
	In/Out	6.5 ± 1.4	1.4 ± 0.3	0.1	0.1	0.8 ± 0.2	0.2 ± 0.1	2.8 ± 0.6	0.5	10.1 ± 2.1	2.2 ± 0.5
	Nit/Metab	—	18.5 ± 1.6	—	11.6 ± 0.9	—	5.2 ± 1.4	—	9.4 ± 2.6	—	44.8 ± 6.6
ΔR	In/Out	62 ± 13	22 ± 5	3 ± 1	6 ± 1	12 ± 2	5	111 ± 23	32 ± 6	188 ± 38	65 ± 13
	Nit/Metab	166 ± 26	279 ± 25	216 ± 18	233 ± 18	166 ± 29	106 ± 29	92 ± 41	146 ± 41	641 ± 113	764 ± 113
ΔN	Dep	9.5 ± 1.7	—	4.9 ± 0.9	—	7.8 ± 1.4	—	14.6 ± 2.6	—	36.9 ± 6.7	—
	In/Out	69 ± 14	24 ± 5	3 ± 1	6 ± 1	13 ± 2	5 ± 1	114 ± 23	32 ± 7	199 ± 40	67 ± 14
	Nit/Metab	166 ± 26	297 ± 27	216 ± 18	245 ± 19	166 ± 29	111 ± 30	92 ± 41	156 ± 44	641 ± 113	809 ± 120

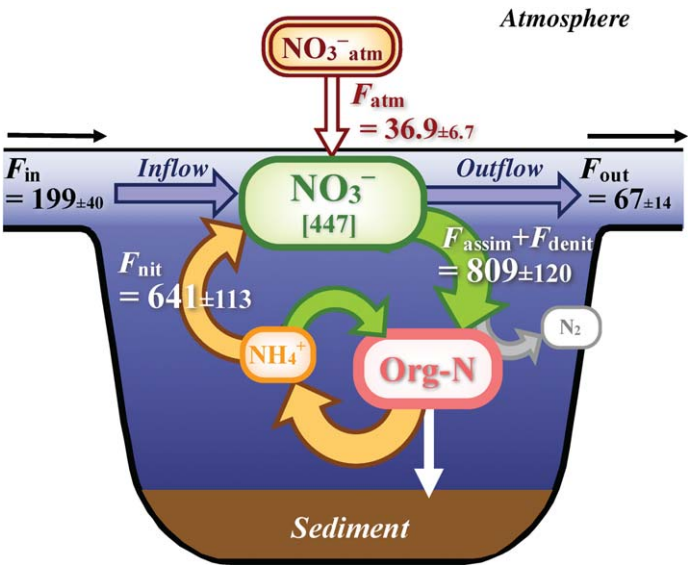

Fig. 4. Schematic diagram showing nitrate cycling dynamics in Lake Biwa as estimated by using the $\Delta^{17}O$ method. The magnitude of the nitrate reservoir in the lake's water column in March is presented in brackets (unit: Mmol = 10^6 mol), together with the estimated annual fluxes between each reservoir (unit: Mmol N yr^{-1} = 10^6 mol N yr^{-1}).

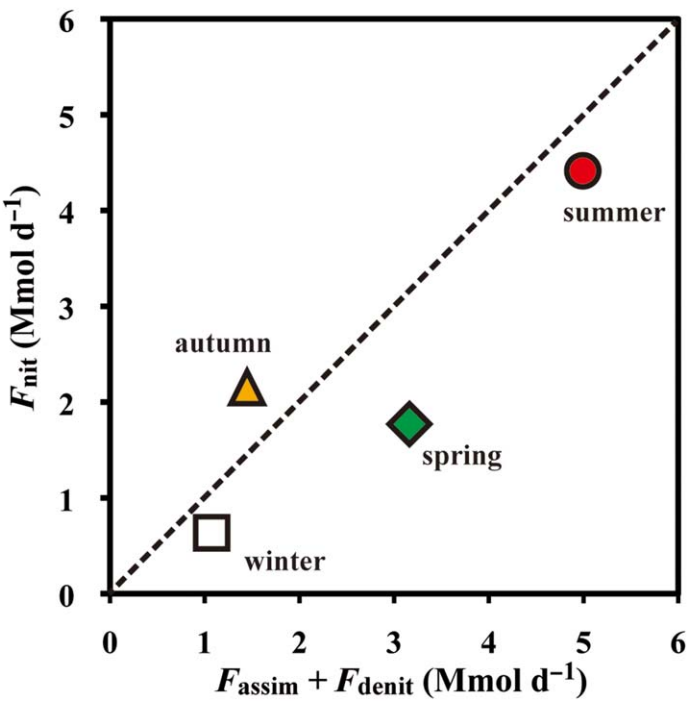

Fig. 5. Relation between the gross metabolic rate ($F_{assim} + F_{denit}$) of nitrate and gross nitrification rate (F_{nit}) determined for each season in Lake Biwa. The dotted line represents the 1 : 1 relation between the corresponding values.

(Fig. 5). This normal correlation between $F_{assim} + F_{denit}$ and F_{nit} implies that F_{nit} in the lake increased in response to the $F_{assim} + F_{denit}$ increase and decreased in response to the $F_{assim} + F_{denit}$ decrease, which corresponds to rapid remineralization of organic nitrogen to NO_3^- in the lake. That is to say, organic nitrogen produced from NO_3^- via assimilation had a short lifetime in the lake's water column, remineralizing to NO_3^- shortly after assimilation.

We also detected a gradual increasing trend in the $F_{nit}/(F_{assim} + F_{denit})$ ratios from spring to autumn (Fig. 5). Whereas the $F_{nit}/(F_{assim} + F_{denit})$ ratio was 0.6 in spring, the $F_{nit}/(F_{assim} + F_{denit})$ ratio increased to 0.9 in summer, and 1.5 in autumn. The gradual increasing trend can be explained well by assuming the average time lag between production of new organic nitrogen through assimilation (= assimilation of NO_3^-) and remineralization to NO_3^- through nitrification was around 1 month, on average, in the lake's water

column. While $F_{nit}/(F_{assim}+F_{denit})$ increased because of blooming in spring, F_{nit} was still low because of the time lag, so that the $F_{nit}/(F_{assim}+F_{denit})$ ratio was low in spring. In summer, when F_{assim} was at the maximum for the year, F_{nit} increased and became comparable with F_{assim}, therefore the $F_{nit}/(F_{assim}+F_{denit})$ ratio was close to 1. While F_{assim} decreased in autumn, F_{nit} remained at a high level because of the time lag, and thus the $F_{nit}/(F_{assim}+F_{denit})$ ratio became higher in autumn.

This average time lag was highly reasonable given the residence time of PON in freshwater environments. For instance, Islam et al. (2013) determined the average decomposition rates for the reactions from natural PON to NO_3^- in rivers under dark conditions and found that the rate-limiting step (from PON to dissolved organic nitrogen) was 0.028 d^{-1}. We concluded that the seasonal variations in F_{nit} and $F_{assim}+F_{denit}$ estimated in this study were highly reliable estimates for the lake.

The total amount of NO_3^- metabolized in the water column for the year (809 ± 120 Mmol; Table 3) was much larger than the total inventory of NO_3^- in the lake's water column in March (447 Mmol; Table 2), as well as the annual influx of NO_3^- via inflows (199 ± 40 Mmol; Table 3) or atmospheric deposition (36.9 ± 6.7 Mmol; Table 3). We concluded that the rapid remineralization (nitrification) in the lake played a major role in sustaining the primary production using NO_3^- within the lake, rather than that from influx via inflows or atmospheric deposition. Dividing the total inventory of NO_3^- in March by the integrated annual removal rates (annual gross metabolic rate in the lake and annual efflux rate via outflows) yielded an approximate residence time of NO_3^- in the lake of 0.5 yr. This residence time corresponds to less than 1/10 of that for the water in the lake.

Comparison with the ^{15}N tracer method

To see if the estimated total metabolic rates of NO_3^- ($F_{assim}+F_{denit}$) using the $\Delta^{17}O$ method were reasonable, we also determined the assimilation rates of NO_3^- (F_{assim}) using the ^{15}N tracer method simultaneously and compared the results between the two. Clear ^{15}N enrichment of more than +200‰ was always observed in the PON samples incubated for 24 h under $^{15}NO_3^-$ addition. The determined gross NO_3^- assimilation rates in the bottles ranged from 90 mmol N L^{-1} d^{-1} to 709 mmol N L^{-1} d^{-1}, and the depth integrated areal gross rates ranged from 4.0 mmol N L^{-1} d^{-1} to 5.2 mmol N d^{-1} m^{-2} (Fig. 6). These values coincided well with those determined using the ^{15}N tracer incubation method in the same lake in past studies (Frenette et al. 1996, 1998).

The estimated annual assimilation rate using the ^{15}N tracer method was 978 Mmol yr^{-1} (= 4.6 mmolNO_3^- m^{-2} d^{-1}), which almost corresponds with the annual metabolic rates using the $\Delta^{17}O$ method (809 ± 120 Mmol yr^{-1} = 3.3 ± 0.5 mmolNO_3^- m^{-2} d^{-1}; Table 3 and Fig. 6), implying that the estimated gross metabolic rates of NO_3^- obtained through

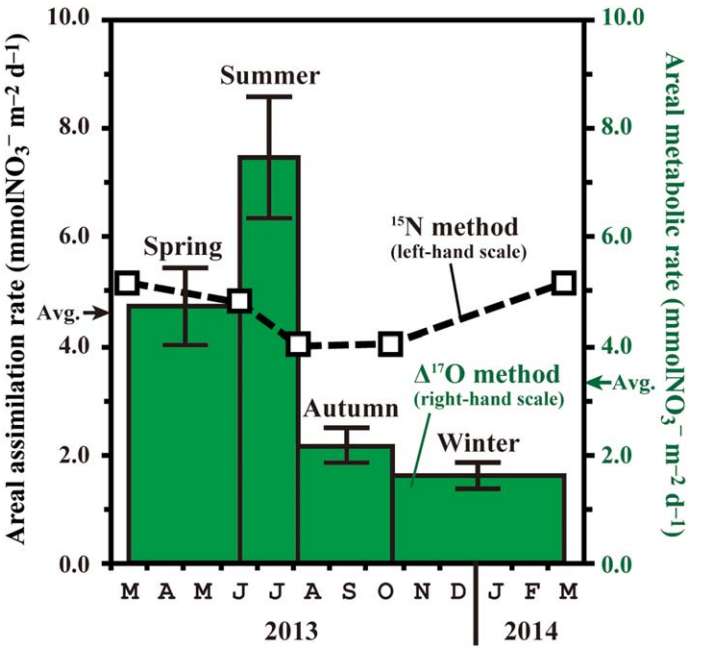

Fig. 6. Temporal variation in the areal assimilation rates of nitrate in Lake Biwa estimated based on the ^{15}N tracer incubation (^{15}N method), shown by white squares and dotted lines using left-hand scale, as well as the areal metabolic rates estimated based on the $\Delta^{17}O$ values of nitrate in the lake's water column ($\Delta^{17}O$ method), shown by colored bars using right-hand scale. The arrow on the left-hand scale represents annual average of the areal assimilation rates estimated based on the ^{15}N method and that on the right-hand scale represents annual average of the areal metabolic rates estimated based on the $\Delta^{17}O$ method.

the use of the $\Delta^{17}O$ method were highly reliable as for the NO_3^- dynamics in the lake. Whereas the metabolic rates of NO_3^- estimated based on the $\Delta^{17}O$ method were the total metabolic rates of NO_3^- ($F_{assim}+F_{denit}$), in which not only those through assimilation (F_{assim}) but also those through denitrification (F_{denit}) were included (Tsunogai et al. 2011), the assimilation rates estimated based on the ^{15}N tracer method corresponded to those through assimilation only (F_{assim}). If denitrification was significant in the lake, the metabolic rates estimated based on the $\Delta^{17}O$ method would have been higher than those estimated based on the ^{15}N tracer method. However, the actual total metabolic rates estimated based on the $\Delta^{17}O$ method showed the opposite trend; smaller than the assimilation rates estimated based on the ^{15}N tracer method by 20% on the annual average. Consequently, the present results also implied that the metabolic rates of NO_3^- through denitrification were much lower than those through assimilation in the lake (i.e., $F_{denit} \ll F_{assim}$). Furthermore, several problems inherent in the two different methods could be responsible for the discrepancies between the results.

These problems include the (1) NO_3^- assimilation by periphyton that had been excluded from the assimilation

rates estimated based on the ^{15}N method using bottles (Axler and Reuter 1996), (2) NO_3^- metabolism in the littoral zone of the lake that had been excluded from the assimilation rates estimated based on the ^{15}N method using bottles (Slawyk et al. 1998), (3) production of $DO^{15}N$ during incubation in the bottles using the ^{15}N tracer method, and (4) occurrence of photoinhibition during water sample handling shipboard for the incubation using the ^{15}N tracer method. However, all of these problems were likely minor because they would have induced higher total metabolic rates in the $\Delta^{17}O$ method than in the ^{15}N tracer method, whereas the results showed the opposite trend (Fig. 6). More likely causes for the discrepancies are (5) artificial stimulation of NO_3^- assimilation rates using the ^{15}N tracer method from possible contamination by trace nutrients (including trace metals) in the bottles and (6) poor representativeness of the determined assimilation rates based on the ^{15}N tracer method for the values representing each season. Because the assimilation rate estimated by using the ^{15}N tracer method was based on the instantaneous assimilation rate at each sampling point, the potential problem described in (6) was most likely responsible for the discrepancies, especially for those in summer and winter.

Because NO_3^- was almost exhausted from the surface 10 m in August (Fig. 3b), the instantaneous assimilation rate determined was inevitably low. The observed NO_3^- depletion in August, however, implies that active NO_3^- assimilation occurred prior to the sampling. As a result, if we take into account the active NO_3^- assimilation prior to the sampling date (i.e., prior to the NO_3^- being exhausted), the actual assimilation rate in summer should be larger than that determined in August based on the ^{15}N tracer method.

In contrast, the instantaneous assimilation rate determined on the sampling days in winter (15 March and 21 October) might be larger than that of the other days in winter. Whereas the solar irradiance levels were lowest in winter, e.g., less than 10 MJ m^{-2} at the surface in general, they were high on the sampling days, e.g., at around 15 MJ m^{-2} and 20 MJ m^{-2}, respectively. In addition, the surface was enriched in nutrients owing to deep convection. Because assimilation rates of NO_3^- are a function of photosynthetically available radiation under low irradiance/high nutrient conditions (Frenette et al. 2003), the NO_3^- assimilation rates might have been higher during sampling in October and March than the typical values for winter. This was partly a result of our attempts to avoid windy or rainy days during lake water sampling to ensure safe boat operations; hence, the solar irradiance levels were higher than normal.

Whatever the specific reasons were, however, all of the possible problems described above are problems inherent in the ^{15}N tracer method and not problems associated with the $\Delta^{17}O$ method. The findings for both the total metabolic rates using the $\Delta^{17}O$ method was higher than the assimilation rates using the ^{15}N tracer incubation method in summer and the total metabolic rates using the $\Delta^{17}O$ method was lower than the assimilation rates using the ^{15}N tracer incubation method in winter also support the notion that the total metabolic rates of NO_3^- based on the $\Delta^{17}O$ method are highly reliable for the studied lake. Thus, we concluded that the estimated total metabolic rates of NO_3^- that were obtained using the $\Delta^{17}O$ method represented accurate values for the lake.

Comparison with the denitrification rates reported in the literatures

As shown in "Comparison with the ^{15}N tracer method" section, the results of the present study implied that, in the lake, the metabolic rates of NO_3^- through denitrification were much lower than those through assimilation ($F_{denit} \ll F_{assim}$). To verify this hypothesis, we compared the total metabolic rates of NO_3^- ($F_{assim} + F_{denit}$) determined for the lake in this study with those through denitrification (F_{denit}) determined for the lake in past studies.

Miyajima (1994) estimated the denitrification rate in the lake as 159 ± 13 Mmol yr^{-1}, based on areal denitrification rates determined directly at the surface of offshore sediments (ranged from 0.08 mmol m^{-2} d^{-1} to 0.16 mmol m^{-2} d^{-1}). Similar areal denitrification rates have been obtained during recent surveys as well (Morita and Maegawa 2006). These denitrification rates correspond to only $20\% \pm 5\%$ of the total metabolic rates of NO_3^- ($F_{assim} + F_{denit}$) estimated based on the $\Delta^{17}O$ method in this study (809 ± 120 Mmol yr^{-1}). We concluded that denitrification was minor within the whole NO_3^- metabolism in the lake, and thus more than 75% of the NO_3^- metabolism ($F_{assim} + F_{denit}$) was through assimilation (F_{assim}).

Whereas dissolved oxygen in the hypolimnion of the lake shows a gradual decreasing trend every year (Kalff 2002), oxygen is still enriched in most of the lake's water column (Shiga Prefecture 2015). The minimum concentration of dissolved oxygen in 2013, for instance, was 39% of the saturation level within the whole monthly monitoring data set collected at offshore stations by Shiga Prefecture (Shiga Prefecture 2015). The relatively slower denitrification rates than the assimilation rates in the lake should be reasonable as the NO_3^- dynamics in the lake.

As presented in the previous section, the estimated assimilation rates (F_{assim}) based on the ^{15}N tracer method were less reliable in this study (as well as in past studies) than the total metabolic rates of NO_3^- ($F_{assim} + F_{denit}$) estimated based on the $\Delta^{17}O$ method, probably because the number of sampling events was insufficient to obtain accurate and precise F_{assim} using the ^{15}N tracer method. If we were to estimate F_{assim} that was more precise and accurate based on the ^{15}N tracer method by increasing the number of sampling events throughout the year, we would be able to estimate denitrification rates (F_{denit}) that were more precise from the difference between F_{assim} obtained through the highly precise ^{15}N

tracer method and $F_{assim} + F_{denit}$ obtained through the $\Delta^{17}O$ method.

Nitrification in the lake's water column

The present study revealed that 245 ± 19 Mmol of NO_3^- had been metabolized in the water column during summer (Table 3). As discussed in "Comparison with the denitrification rates reported in the literatures" section, more than 75% of the NO_3^- metabolism (184 ± 19 Mmol or more) was via assimilation (primary production), so it must have occurred in the surface 15 m of the lake (Urabe et al. 1999). However, net NO_3^- loss in the shallow layers (from 0 m to 30 m depth, which almost corresponds to the epilimnion and thermocline in summer) during summer was only 19 Mmol (Table 2), thus the calculations show a shortage of 165 ± 19 Mmol or more for NO_3^-. Possible supply processes for NO_3^- in the shallow layers of the lake include upwelling (i.e., vertical transportation) from deep layers (from 30 m depth to the bottom, which almost corresponds to the hypolimnion in summer), influx via rivers, atmospheric deposition, and in situ nitrification within the shallow layers. Even considering the net NO_3^- inputs via inflows (-3 ± 2 Mmol in net value; Table 3) and atmospheric deposition (4.9 ± 0.9 Mmol; Table 3) during summer to the shallow layers, a shortage of 163 ± 19 Mmol or more for NO_3^- existed. In a similar manner, shortages of 59 ± 27 Mmol, 100 ± 30 Mmol, and 118 ± 44 Mmol for NO_3^- were found during spring, autumn, and winter, respectively, which must have been supplied to the shallow layers either through upwelling from the deeper layers and/or in situ nitrification.

The upwelling of NO_3^- from the deep to shallow layers provides a reasonable explanation in winter when the surface mixed layer developed because of cooling at the surface. Similar upwelling could be anticipated for both early spring and late autumn. As for the summer, when the lake water stratified and the thermocline extended from 12 m to 30 m depth (Fig. 3a), however, it is difficult to assume that upwelling of NO_3^- from the hypolimnion over the thermocline was responsible for the observed shortage. Even using the possible maximum vertical eddy diffusivity in the thermocline (10^{-5} m^2 s^{-1}) (Etemad-Shahidi and Imberger 2006), vertical transport only corresponded to 28 Mmol in summer. As a result, we must assume that nitrification in the surface 15 m (epilimnion and upper thermocline) supplied the NO_3^- needed for the assimilation.

Until the 1990s, nitrification was believed to occur almost entirely in the deep aphotic zone, possibly because of inhibition by light (Horrigan and Springer 1990; Guerrero and Jones 1996). Recent studies on NO_3^- in the subtropical ocean, however, revealed that a substantial fraction of NO_3^- assimilation involves NO_3^- that was regenerated through nitrification near the surface at depths around the upper thermocline (Yool et al. 2007).

The ^{15}N-depleted NO_3^- found in the present study at depths of around 10–20 m in June, August, and October, relative to that in the deeper layers (Fig. 3d), is also indicative of the influence of shallow nitrification at depth in the lake. In March, the $\delta^{15}N$ values were almost uniform at $+5.0 \pm 0.2$‰, irrespective of the depth. On the other hand, definitively ^{15}N-depleted $\delta^{15}N$ values as low as +3.5‰ were found in the upper thermocline (depth = 20 m) in June. These values had decreased from a maximum of +7.0‰ at the hypolimnion. In August, we observed much lower $\delta^{15}N$ values of +1.4‰ at 15 m, which was in the upper thermocline, that decreased from a maximum of +10.4‰ in the hypolimnion. In October, the $\delta^{15}N$ values were nearly uniform at $+5.6 \pm 1.7$‰, irrespective of the depth again, which was probably due to the active vertical convection of water in autumn. Still, we found a more ^{15}N-depleted $\delta^{15}N$ value of +3.8‰ at the 5 m depth.

Because partial progression of assimilation and/or denitrification fractionate the residual NO_3^- so that it becomes enriched in both ^{15}N and ^{18}O, it is difficult to assume that NO_3^- in the deep layers ($\delta^{15}N = +5.1$‰ in March, +6.0‰ in June, +7.9‰ in August, and +7.5‰ in October) was the major source of the ^{15}N-depleted NO_3^- in the upper thermocline in the lake (as low as +3.5‰ in June, +1.4‰ in August, and +3.8‰ in October). Additionally, it is difficult to assume river input as the source of the ^{15}N-depleted NO_3^- because NO_3^- in inflows had higher $\delta^{15}N$ values ($\delta^{15}N = +4.0$‰ in March, +6.8‰ in June, +5.6‰ in August, and +5.6‰ in October on average; Tsunogai et al. 2016) than the ^{15}N-depleted NO_3^-. Similar ^{15}N-depleted NO_3^-, relative to that in the deeper layers, was found in the subtropical ocean, and this was recognized as evidence of in situ nitrification producing more ^{15}N-deleted NO_3^- in the shallow layers than nitrification in the deeper layers (Casciotti et al. 2008). We concluded that the ^{15}N-depleted NO_3^- found at depths around the upper thermocline relative to that in the deeper layers had been produced through in situ nitrification, probably through alterations of fresh, sinking PON.

The $\delta^{15}N$ values of seston in the surface water (0–10 m depths; Fig. 3f) also support this conclusion. Whereas the $\delta^{15}N$ values of seston were around +10‰ in March, they decreased to +4‰ in June, implying that the $\delta^{15}N$ values of fresh seston (i.e., sinking particles) in the lake column were less than +4‰. In addition, relative ^{15}N-enrichment of seston in the hypolimnion compared to the surface implied that kinetic isotope effects were significant for $\delta^{15}N$ during nitrification. That is to say, $\delta^{15}N$ values of NO_3^- produced through nitrification should be lower than those of sinking PON. As a result, ^{15}N-depleted fresh seston is the most probable source for the ^{15}N-depleted NO_3^- found at depth around the upper thermocline.

Tezuka (1986) collected seston from the water column of Lake Biwa at several depths during the summer of 1985 and let the samples incubate under aerobic conditions,

simulating those of the lake water, for 3 months. Through the experiments, they found significant liberation of NO_3^- from seston, especially from fresh seston collected at the depth of 5 m, from which almost all fixed *N* had been converted to NO_3^- within 40 d. His results, including the time needed for decomposition (as already presented in "Quantifying nitrate dynamics between each observation" section), coincided well with our observations. Thus, we concluded that most of the shortage found for NO_3^- in the shallow layers had been supplied through in situ nitrification in the epilimnion and upper thermocline, at least in summer.

Comparison with dynamics of P in the lake

Yoshimizu et al. (2002) determined the budgets for P nutrients in Lake Biwa and estimated that input via inflows occupied 56% of the total P metabolized in the lake's water column; thus, remineralized P occupied only 44%. For the NO_3^- determined in this study, input via inflows occupied only 24% of the total NO_3^- metabolized in the lake while nitrification (i.e., $NO_{3\,re}^-$) corresponded to 79% (Fig. 4). When we take into account recycling via ammonium, the recycling of total N nutrients must be much larger than 79% in the lake (Fig. 4). Therefore, in-lake remineralization of N must be an important process that maintains primary production in the lake. Similar results were also implied in decomposition experiments with seston in the lake (Tezuka 1986). While inorganic N nutrients were quickly released from seston at a time scale of 1 month, most of the P was retained in the seston. As a result, most of the P in the seston settled to the bottom and was fixed in the sediments of the lake. Whereas remineralization rates of organic P can be higher than organic N in general (Islam et al. 2013), the relationship was the opposite in Lake Biwa. The annual input of total fixed N from external sources such as inflows and atmospheric deposition was estimated to be around 350 Mmol yr^{-1} (Kunimatsu 1995), and that of P was estimated to be around 29 Mmol yr^{-1} (Yoshimizu et al. 2002). Therefore, the inflows of Lake Biwa can be characterized by relative P enrichment, having lower N/P ratios (around 12) than the Redfield ratio (around 16). This relative P enrichment in the inflows of Lake Biwa might be responsible for the characteristic lake ecosystem, which uses N nutrients effectively through remineralization in the water column.

Concluding remarks

By using the $\Delta^{17}O$ values of NO_3^- dissolved in Lake Biwa, the present study revealed that NO_3^- supplied by inflows occupied only less than 30% of the NO_3^- in the lake. Thus, in-lake nitrification is the major source of NO_3^-, as schematically shown in Fig. 4. Besides, most NO_3^- that was metabolized in spring and summer was supplied through in situ nitrification within the epilimnion and upper thermocline. Furthermore, about 80% of the metabolized NO_3^- was remineralized to NO_3^- again via rapid turnover of NO_3^- in the lake at a time scale of 1 month, implying that the metabolic process was mostly assimilation (i.e., primary production).

The $\Delta^{17}O$ method presented in this study can be an alternative to standard techniques that use ^{15}N tracers for the accurate determination of gross nitrification rates (F_{nit}) and gross total metabolic rates of NO_3^- ($F_{assim} + F_{denit}$) in aquatic environments that contain detectable quantities of $NO_{3\,atm}^-$ within the total NO_3^- pool. Besides, in contrast to the snapshot tracer approach, the $\Delta^{17}O$ method integrated long-term changes, so that we can deduce changes in NO_3^- dynamics for a period without observation. By combining data on NO_3^- dynamics obtained through the $\Delta^{17}O$ method with data from the most recent advanced techniques to measure accurate and precise gross primary production rates simultaneously, we will be able to clarify biogeochemical dynamics in each aquatic environment more accurately, including regarding temporal variation.

As presented in Eq. 7, the uncertainties in the estimated NO_3^- dynamics (i.e., uncertainties in the estimated ΔN_{nit} and thus $\Delta N_{assim} + \Delta N_{denit}$) were primarily determined by the uncertainties in the integrated amount of $NO_{3\,atm}^-$ supplied to the lake water during the period studied ($+\Delta A_{in} - \Delta A_{out} + \Delta N_{atm}$), under the observed small $\Delta^{17}O_{lake}$ values of around $+1‰$ in the lake water. Because the deposition rate of $NO_{3\,atm}^-$ to the lake surface (ΔN_{atm}) was much larger than the influx/efflux of $NO_{3\,atm}^-$ via streams (ΔA_{in} and ΔA_{out}) in Lake Biwa (Table 3), the uncertainties in the estimated NO_3^- dynamics were primarily derived from those in the deposition rate of $NO_{3\,atm}^-$ (ΔN_{atm}). This was the case for Lake Mashu as well (Tsunogai et al. 2011). The shortest interval between observations was 49 d in this study. Whereas the variation in both the concentrations and $\Delta^{17}O$ values between the observations was large enough to quantify temporal variation of NO_3^- in the lake's water column (Table 2), the interval was close to the minimum interval for obtaining reliable deposition amounts of $NO_{3\,atm}^-$ (ΔN_{atm}). As a result, we should be able to attain better precision and accuracy in the values of F_{nit} and $F_{assim} + F_{denit}$ estimated for a lake in general, if we could enhance both the precision and accuracy of the deposition rate for $NO_{3\,atm}^-$ in the lake (F_{atm}). That is to say, we will be able to enhance both the precision and accuracy of F_{nit} and $F_{assim} + F_{denit}$ through monitoring the deposition rate of $NO_{3\,atm}^-$ at several observatories around the lake, rather than intensified monitoring in the lake itself.

References

Aleem, M. I. H., G. E. Hoch, and J. E. Varner. 1965. Water as the source of oxidant and reductant in bacterial chemosynthesis. Proc. Natl. Acad. Sci. USA **54**: 869–873. doi: 10.1073/pnas.54.3.869

Alexander, B., M. G. Hastings, D. J. Allman, J. Dachs, J. A. Thornton, and S. A. Kunasek. 2009. Quantifying atmospheric nitrate formation pathways based on a global model of the oxygen isotopic composition ($\Delta^{17}O$) of

atmospheric nitrate. Atmos. Chem. Phys. **9**: 5043–5056. doi:10.5194/acp-9-5043-2009

Andersson, K. K., and A. B. Hooper. 1983. O_2 and H_2O are each the source of one O in NO_2^- produced from NH_3 by *Nitrosomonas*: ^{15}N-NMR evidence. FEBS Lett. **164**: 236–240. doi:10.1016/0014-5793(83)80292-0

Axler, R. P., and J. E. Reuter. 1996. Nitrate uptake by phytoplankton and periphyton: Whole-lake enrichments and mesocosm-N-15 experiments in an oligotrophic lake. Limnol. Oceanogr. **41**: 659–671. doi:10.4319/lo.1996.41.4.0659

Böhlke, J. K., and T. B. Coplen. 1995. Interlaboratory comparison of reference materials for nitrogen-isotope-ratio measurements, p. 51–66. *In* Reference and intercomparison materials for stable isotopes of light elements. Proceedings of a consultants meeting held in Vienna, 01–03 December 1993. IAEA-TECDOC-825. IAEA.

Böhlke, J. K., S. J. Mroczkowski, and T. B. Coplen. 2003. Oxygen isotopes in nitrate: New reference materials for ^{18}O:^{17}O:^{16}O measurements and observations on nitrate-water equilibration. Rapid Commun. Mass Spectrom. **17**: 1835–1846. doi:10.1002/rcm.1123

Casciotti, K. L., T. W. Trull, D. M. Glover, and D. Davies. 2008. Constraints on nitrogen cycling at the subtropical North Pacific Station ALOHA from isotopic measurements of nitrate and particulate nitrogen. Deep-Sea Res. Part II Top. Stud. Oceanogr. **55**: 1661–1672. doi:10.1016/j.dsr2.2008.04.017

Duce, R. A., and others. 2008. Impacts of atmospheric anthropogenic nitrogen on the open ocean. Science **320**: 893–897. doi:10.1126/science.1150369

Dugdale, R. C., and J. J. Goering. 1967. Uptake of new and regenerated forms of nitrogen in primary productivity. Limnol. Oceanogr. **12**: 196–206. doi:10.4319/lo.1967.12.2.0196

EANET. 2014. Data report 2013. Network center for EANET (acid deposition monitoring network in East Asia), Asia Center for Air Pollution Research.

Elser, J. J., and others. 2009. Shifts in lake N:P stoichiometry and nutrient limitation driven by atmospheric nitrogen deposition. Science **326**: 835–837. doi:10.1126/science.1176199

Environmental Laboratories Association in Japan. 2015. Reports on the 5th national survey on acid rain (FY2013). J. Environ. Lab. Assoc. **40**: 98–142.

Etemad-Shahidi, A., and J. Imberger. 2006. Diapycnal mixing in the thermocline of lakes: Estimations by different methods. Environ. Fluid Mech. **6**: 227–240. doi:10.1007/s10652-005-4480-6

Frenette, J.-J., W. F. Vincent, L. Legendre, and T. Nagata. 1996. Size-dependent phytoplankton responses to atmospheric forcing in Lake Biwa. J. Plankton Res. **18**: 371–391. doi:10.1093/plankt/18.3.371

Frenette, J.-J., W. F. Vincent, and L. Legendre. 1998. Size-dependent C:N uptake by phytoplankton as a function of irradiance: Ecological implications. Limnol. Oceanogr. **43**: 1362–1368. doi:10.4319/lo.1998.43.6.1362

Granger, J., D. M. Sigman, M. M. Rohde, M. T. Maldonado, and P. D. Tortell. 2010. N and O isotope effects during nitrate assimilation by unicellular prokaryotic and eukaryotic plankton cultures. Geochim. Cosmochim. Acta **74**: 1030–1040. doi:10.1016/j.gca.2009.10.044

Guerrero, M. A., and R. D. Jones. 1996. Photoinhibition of marine nitrifying bacteria 1. Wavelength-dependent response. Mar. Ecol. Prog. Ser. **141**: 183–192. doi:10.3354/meps141183

Hayakawa, K., S. Tsujimura, T. Ishikawa, H. Haga, T. Okamoto, C. Jiao, K. Ishikawa, and M. Kumagai. 2012. Long-term changes in the concentrations of total phosphorus and nitrate in some quality parameters of water in Lake Biwa using integrated analysis from several monitoring data [in Japanese with English abstract]. J. Jpn. Soc. Water Environ. **35**: 89–100. doi:10.2965/jswe.35.89

Hirota, A., U. Tsunogai, D. D. Komatsu, and F. Nakagawa. 2010. Simultaneous determination of δ^{15}N and δ^{18}O of N_2O and δ^{13}C of CH_4 in nanomolar quantities from a single water sample. Rapid Commun. Mass Spectrom. **24**: 1085–1092. doi:10.1002/rcm.4483

Horrigan, S. G., and A. L. Springer. 1990. Oceanic and estuarine ammonium oxidation: Effects of light. Limnol. Oceanogr. **35**: 479–482. doi:10.4319/lo.1990.35.2.0479

Hsieh, C. H., Y. Sakai, S. Ban, K. Ishikawa, T. Ishikawa, S. Ichise, N. Yamamura, and M. Kumagai. 2011. Eutrophication and warming effects on long-term variation of zooplankton in Lake Biwa. Biogeosciences **8**: 1383–1399. doi:10.5194/bgd-8-593-2011

Islam, M. J., and others. 2013. The decomposition rates of organic phosphorus and organic nitrogen in river waters. J. Fresh. Ecol. **28**: 239–250. doi:10.1080/02705060.2012.733969

Kaiser, J., M. G. Hastings, B. Z. Houlton, T. Röckmann, and D. M. Sigman. 2007. Triple oxygen isotope analysis of nitrate using the denitrifier method and thermal decomposition of N_2O. Anal. Chem. **79**: 599–607. doi:10.1021/ac061022s

Kalff, J. 2002. Limnology: Inland water ecosystems. Prentice Hall.

Knap, A., A. Michaels, A. Close, H. Ducklow, and A. Dickson. 1996. Protocols for the Joint Global Ocean Flux Study (JGOFS) core measurements, p. 170. Reprint of the IOC manuals and guides no. 29. UNESCO, 1994. Scientific Committee on Oceanic Research, International Council of Scientific Unions.

Komatsu, D. D., T. Ishimura, F. Nakagawa, and U. Tsunogai. 2008. Determination of the ^{15}N/^{14}N, ^{17}O/^{16}O, and ^{18}O/^{16}O ratios of nitrous oxide by using continuous-flow isotope-ratio mass spectrometry. Rapid Commun. Mass Spectrom. **22**: 1587–1596. doi:10.1002/rcm.3493

Konno, U., and others. 2010. Determination of total N_2 fixation rates in the ocean taking into account both the particulate and filtrate fractions. Biogeosciences **7**: 2369–2377. doi:10.5194/bgd-7-765-2010

Kumar, S., D. J. D. Nicholas, and E. H. Williams. 1983. Definitive ^{15}N NMR evidence that water serves as a source of 'O' during nitrite oxidation by *Nitrobacter agilis*. FEBS Lett. **152**: 71–74. doi:10.1016/0014-5793(83)80484-0

Kunimatsu, T. 1995. Mass balance of Lake Biwa [in Japanese]. LBRI Bull. **12**: 68–73.

McIlvin, M. R., and M. A. Altabet. 2005. Chemical conversion of nitrate and nitrite to nitrous oxide for nitrogen and oxygen isotope analysis in freshwater and seawater. Anal. Chem. **77**: 5589–5595. doi:10.1021/ac050528s

Michalski, G., J. Savarino, J. K. Böhlke, and M. Thiemens. 2002. Determination of the total oxygen isotopic composition of nitrate and the calibration of a $\Delta^{17}O$ nitrate reference material. Anal. Chem. **74**: 4989–4993. doi:10.1021/ac0256282

Michalski, G., Z. Scott, M. Kabiling, and M. H. Thiemens. 2003. First measurements and modeling of $\Delta^{17}O$ in atmospheric nitrate. Geophys. Res. Lett. **30**: 1870. doi:10.1029/2003GL017015

Michalski, G., T. Meixner, M. Fenn, L. Hernandez, A. Sirulnik, E. Allen, and M. Thiemens. 2004. Tracing atmospheric nitrate deposition in a complex semiarid ecosystem using $\Delta^{17}O$. Environ. Sci. Technol. **38**: 2175–2181. doi:10.1021/es034980+

Miller, M. F. 2002. Isotopic fractionation and the quantification of ^{17}O anomalies in the oxygen three-isotope system: An appraisal and geochemical significance. Geochim. Cosmochim. Acta **66**: 1881–1889. doi:10.1016/S0016-7037(02)00832-3

Mitamura, N. 2014. Analysis on variation of nitrogen dry deposition [in Japanese]. J. Environ. Lab. Assoc. **39**: 25–30.

Miyajima, T. 1994. Mud-water fluxes of inorganic nitrogen and manganese in the pelagic region of Lake Biwa: Seasonal dynamics and impact on the hypolimnetic metabolism. Arch. Hydrobiol. **130**: 303–324.

Morin, S., J. Savarino, M. M. Frey, N. Yan, S. Bekki, J. W. Bottenheim, and J. M. F. Martins. 2008. Tracing the origin and fate of NO_X in the Arctic atmosphere using stable isotopes in nitrate. Science **322**: 730–732. doi:10.1126/science.1161910

Morita, T., and T. Maegawa. 2006. Denitrification activity in sediments from Lake Biwa [in Japanese]. Bull. Shiga Prefect. Fish. Exp. Stn. **51**: 1–9.

Nakagawa, F., U. Tsunogai, T. Gamo, and N. Yoshida. 2004. Stable isotopic compositions and fractionations of carbon monoxide at coastal and open ocean stations in the Pacific. J. Geophys. Res. **109**: C06016. doi:10.1029/2001JC001108

Nakagawa, F., A. Suzuki, S. Daita, T. Ohyama, D. D. Komatsu, and U. Tsunogai. 2013. Tracing atmospheric nitrate in groundwater using triple oxygen isotopes: Evaluation based on bottled drinking water. Biogeosciences **10**: 3547–3558. doi:10.5194/bg-10-3547-2013

Ohte, N., and others. 2010. Spatial distribution of nitrate sources of rivers in the Lake Biwa watershed, Japan: Controlling factors revealed by nitrogen and oxygen isotope values. Water Resour. Res. **46**: W07505. doi:10.1029/2009wr007871

Ota, Y., N. Goto, and S. Ban. 2013. Estimation of in situ primary productivity using chlorophyll fluorescence technique in phytoplankton and its verification [in Japanese with English abstract]. Jpn. J. Limnol. **74**: 173–181. doi:10.3739/rikusui.74.173

Santoro, A. E., K. L. Casciotti, and C. A. Francis. 2010. Activity, abundance and diversity of nitrifying archaea and bacteria in the central California Current. Environ. Microbiol. **12**: 1989–2006. doi:10.1111/j.1462-2920.2010.02205.x

Shiga Prefecture. 2015. Annual report on the environment in Shiga (FY 2013), Appendix [in Japanese]. Shiga prefecture.

Slawyk, G., P. Raimbault, and N. Garcia. 1998. Measuring gross uptake of N-15-labeled nitrogen by marine phytoplankton without particulate matter collection: Evidence of low N-15 losses to the dissolved organic nitrogen pool. Limnol. Oceanogr. **43**: 1734–1739. doi:10.4319/lo.1998.43.7.1734

Tezuka, Y. 1986. Does the seston of Lake Biwa release dissolved inorganic nitrogen and phosphorus during aerobic decomposition? Its implication for eutrophication. Ecol. Res. **1**: 293–302. doi:10.1007/BF02348686

Tsunogai, U., N. Yoshida, J. Ishibashi, and T. Gamo. 2000. Carbon isotopic distribution of methane in deep-sea hydrothermal plume, Myojin Knoll Caldera, Izu-Bonin arc: Implications for microbial methane oxidation in ocean and applications to heat flux estimation. Geochim. Cosmochim. Acta **64**: 2439–2452. doi:10.1016/S0016-7037(00)00374-4

Tsunogai, U., F. Nakagawa, D. D. Komatsu, and T. Gamo. 2002. Stable carbon and oxygen isotopic analysis of atmospheric carbon monoxide using continuous-flow isotope ratio MS by isotope monitoring of CO. Anal. Chem. **74**: 5695–5700. doi:10.1021/ac020290x

Tsunogai, U., F. Nakagawa, T. Gamo, and J. Ishibashi. 2005. Stable isotopic compositions of methane and carbon monoxide in the Suiyo hydrothermal plume, Izu-Bonin arc: Tracers for microbial consumption/production. Earth Planet. Sci. Lett. **237**: 326–340. doi:10.1016/j.epsl.2005.05.042

Tsunogai, U., T. Kido, A. Hirota, S. B. Ohkubo, D. D. Komatsu, and F. Nakagawa. 2008. Sensitive determinations of stable nitrogen isotopic composition of organic nitrogen through chemical conversion into N_2O. Rapid Commun. Mass Spectrom. **22**: 345–354. doi:10.1002/rcm.3368

Tsunogai, U., D. D. Komatsu, S. Daita, G. A. Kazemi, F. Nakagawa, I. Noguchi, and J. Zhang. 2010. Tracing the fate of atmospheric nitrate deposited onto a forest ecosystem in eastern Asia using $\Delta^{17}O$. Atmos. Chem. Phys. **10**: 1809–1820. doi:10.5194/acp-10-1809-2010

Tsunogai, U., S. Daita, D. D. Komatsu, F. Nakagawa, and A. Tanaka. 2011. Quantifying nitrate dynamics in an oligotrophic lake using $\Delta^{17}O$. Biogeosciences **8**: 687–702. doi:10.5194/bg-8-687-2011

Tsunogai, U., and others. 2014. Quantifying the effects of clear-cutting and strip-cutting on nitrate dynamics in a forested watershed using triple oxygen isotopes as tracers. Biogeosciences **11**: 5411–5424. doi:10.5194/bg-11-5411-2014

Tsunogai, U., T. Miyauchi, T. Ohyama, D. D. Komatsu, F. Nakagawa, Y. Obata, K. Sato, and T. Ohizumi. 2016. Accurate and precise quantification of atmospheric nitrate in streams draining land of various uses by using triple oxygen isotopes as tracers. Biogeosciences **13**: 3441–3459. doi:10.5194/bg-13-3441-2016

Urabe, J., and others. 1999. Light, nutrients and primary productivity in Lake Biwa: An evaluation of the current ecosystem situation. Ecol. Res. **14**: 233–242. doi:10.1046/j.1440-1703.1999.143300.x

Urabe, J., and others. 2005. The production-to-respiration ratio and its implication in Lake Biwa, Japan. Ecol. Res. **20**: 133–141. doi:10.1007/s11284-005-0052-y

Vet, R., and others. 2014. A global assessment of precipitation chemistry and deposition of sulfur, nitrogen, sea salt, base cations, organic acids, acidity and pH, and phosphorus. Atmos. Environ. **93**: 101–116. doi:10.1016/j.atmosenv.2013.10.060

Yamazaki, A., T. Watanabe, and U. Tsunogai. 2011. Nitrogen isotopes of organic nitrogen in reef coral skeletons as a proxy of tropical nutrient dynamics. Geophys. Res. Lett. **38**: L19605. doi:10.1029/2011GL049053

Yool, A., A. P. Martin, C. Fernández, and D. R. Clark. 2007. The significance of nitrification for oceanic new production. Nature **447**: 999–1002. doi:10.1038/nature05885

Yoshimizu, C., J. Urabe, M. Sugiyama, M. Maruo, E. Nakayama, and M. Nakanishi. 2002. Carbon and phosphorus budgets in the pelagic area of Lake Biwa, the largest lake in Japan. Verh. Int. Verein. Limnol. **28**: 1409–1414. doi:10.1080/03680770.2001.11902687

Acknowledgments

We thank Shin-ichi Nakano, Tadatoshi Koitatabashi, Yukiko Goda, and Tetsuji Akatsuka and the other staff of the Center for Ecological Research, Kyoto University, for their valuable support during the field study in Lake Biwa, which employed the research vessel HASU. We also thank Kosuke Ikeya, Chiho Sukigara, Hiroki Sakuma, Sho Minami, Kenta Ando, Shuichi Hara, Toshiyuki Matsushita, Takahiro Mihara, Teresa Fukuda, Yoshiumi Matsumoto, Rei Nakane, Lin Cheng, Yusuke Obata, Yuuko Nakano, and the other present/past members of the Biogeochemistry Group at Nagoya University for their valuable support during the field study. We thank the anonymous reviewers for valuable remarks on an earlier version of the manuscript. The present study was conducted using joint usage facilities at the Center for Ecological Research, Kyoto University. This work was supported by a Grant-in-Aid for Scientific Research from the Ministry of Education, Culture, Sports, Science, and Technology of Japan under grant 17H00780, 26241006, 16K14308, and 15H02804.

Conflict of Interest

None declared.

Submitted 22 July 2017
Revised 29 September 2017; 20 November 2017
Accepted 05 December 2017

Associate editor: Maren Voss